



ELSEVIER

Nuclear Physics B 592 [FS] (2001) 512–562

NUCLEAR
PHYSICS B

www.elsevier.nl/locate/npe

Flow equation approach to the sine-Gordon model

Stefan Kehrein *

Lyman Laboratory of Physics, Harvard University, Cambridge, MA 02138, USA

Received 28 June 2000; accepted 8 August 2000

Abstract

A continuous sequence of infinitesimal unitary transformations is used to diagonalize the quantum sine-Gordon model for $\beta^2 \in (2\pi, \infty)$. This approach can be understood as an extension of perturbative scaling theory since it links weak- to strong-coupling behavior in a systematic expansion: a small expansion parameter is identified and this parameter remains small throughout the entire flow unlike the diverging running coupling constant of perturbative scaling. Our approximation consists in neglecting higher orders in this small parameter. We find very accurate results for the single-particle/hole spectrum in the strong-coupling phase and can describe the full crossover from weak to strong-coupling. The integrable structure of the sine-Gordon model is not used in our approach. Our new method should be of interest for the investigation of nonintegrable perturbations and for other strong-coupling problems. © 2001 Elsevier Science B.V. All rights reserved.

PACS: 71.10.Pm; 11.10.Hi; 11.10.Gh

Keywords: Flow equations; Renormalization group; Strong-coupling behavior

This work is dedicated to Prof. Wegner on the occasion of his 60th birthday

1. Introduction

1.1. Motivation

Perturbative scaling theory plays a key role for analyzing the large class of physical systems with a mismatch between the high-energy scale of the model and the experimentally interesting low-energy scale. For example, in field theory one is generally interested in the universal properties at energies much lower than the UV (ultraviolet)-cutoff, or in condensed matter physics in energies and temperatures much smaller than the Fermi energy/temperature usually of order of a few 1000 K. In order to link high-energy and low-energy regimes it is of fundamental importance to perform perturbation theory in a *stable* order by first analyzing the effect from high-energy scales, and then progressively smaller

* Present address: Theoretische Physik III, Universität Augsburg, 86135 Augsburg, Germany.

E-mail address: stefan.kehrein@physik.uni-augsburg.de (S. Kehrein).

energies. An elementary example for this procedure is provided by atomic physics, where one, e.g., first establishes the fine structure of a spectrum before using these states to evaluate the hyperfine splittings.

For systems with continuous energy scales, like in field theory, the above observations have led to the development of *perturbative scaling theory*. Perturbative scaling ideas have become a key theoretical tool for analyzing physical systems with many degrees of freedom. The principal idea is to study *perturbatively* the effect of lowering the high-energy cutoff by finding a Hamiltonian with this reduced cutoff and renormalized couplings that describe the same low-energy physics as the original Hamiltonian. In a path integral formulation this is conveniently achieved by successively integrating out the high-energy degrees of freedom.

This procedure leads to the well-known renormalization group (RG) equations that describe the flow of the running coupling constants upon lowering the UV-cutoff. For the important class of *strong-coupling* problems, however, the RG-equations lead to running coupling constants that grow larger and larger at smaller energy scales (and often eventually even diverge). Since the RG-equations themselves are derived perturbatively, this means that the perturbative scaling approach breaks down for strong-coupling problems. Well-known examples for this class of models are the Kondo model in condensed matter physics or QCD in elementary particle physics. In spite of its eventual breakdown, perturbative scaling can still contribute significantly to the understanding of strong-coupling problems. For example, in the Kondo model, the divergence of the running coupling constant occurs at an energy that sets the low-energy Kondo scale of the model, which already allows considerable insight into the problem. Still the approach becomes uncontrolled since the coupling constants grow very large, and it has, so far, not been possible to extend the perturbative scaling approach in such a way that a controlled systematic expansion emerges that links weak- to strong-coupling behavior. One can sum up these observations by noting that the perturbative scaling approach often allows us to identify the relevant low-energy scale of a strong-coupling problem, but frequently not the physical behavior associated with this energy scale or the *crossover* behavior linking high and low energies. For an excellent review of these issues see Ref. [1].

This paper will exemplify the way in which Wegner's method of *flow equations* [2] can overcome these shortcomings and provide an analytic description for a weak- to strong-coupling behavior crossover. In the flow equation approach, a continuous sequence of infinitesimal unitary transformations is applied to a many-particle Hamiltonian such that the Hamiltonian becomes successively more diagonal. Wegner has set up this approach in a differential formulation

$$\frac{dH}{dB} = [\eta(B), H(B)]. \quad (1)$$

Here $\eta(B) = -\eta(B)^\dagger$ is an anti-Hermitian operator. Therefore $H(B)$ as obtained by the solution of this differential equation describes a one-parameter family of unitarily equivalent Hamiltonians. $H(B=0) = H$ is the initial condition relating us to the original Hamiltonian H in which we are interested. *We want $H(B=\infty)$ to be diagonal.* In order to achieve this, Wegner has proposed a suitable choice for the generator $\eta(B)$ that we will

discuss in more detail in Section 3.1. Wegner's construction of η generates a Hamiltonian flow where the interaction matrix elements that couple degrees of freedom with a large energy difference are removed first (for smaller B), and more degenerate matrix elements during later stages of the flow. This *separation of energy scales* is reminiscent of the perturbative scaling approach and allows a stable sequence of approximations. As opposed to the perturbative scaling approach, however, degrees of freedom are *not* integrated out in the flow equation approach, instead they are successively diagonalized. A similar framework that contains Wegner's flow equations as a special case has independently been developed by Głazek and Wilson (*similarity renormalization scheme*) [3,4].

So far the flow equation approach has been applied to a variety of models in condensed matter theory like the n -orbital model [2,5], impurity models like the spin-boson model [6,7] and the Anderson impurity model [8], electron-phonon systems [9,11] and spin models [12,13] etc. (for an overview see also Ref. [14]). One advantage of this scheme lies in the observation that it is a non-perturbative approach due to the separation of energy scales, but still has access to all energy scales since no degrees of freedom are integrated out. Therefore one can investigate correlation functions on all energy scales [6,7]. Also the flow equation approach allows the systematic derivation of low-energy effective Hamiltonians not plagued with singular interactions that frequently occur in other approaches [8–10].

However, these applications did not deal with strong-coupling problems as defined above, which would be a very interesting perspective for this new method. Głazek and Wilson undertook a first step in this direction in Ref. [15]. They investigated a quadratic Hamiltonian that shows strong-coupling behavior due to the formation of a bound state from a continuum, and demonstrated how this model can be solved using infinitesimal unitary transformations. However, since they dealt with a quadratic Hamiltonian, this was not a true many-particle strong-coupling problem as would be of most interest in condensed matter theory or high energy theory.

Recently, I described the application of the flow equation method to the one-dimensional quantum sine-Gordon model [16]. The sine-Gordon model is a many-particle problem with an interesting phase structure including a strong-coupling regime. It was shown in Ref. [16] that it is possible to use the flow equation scheme to develop a systematic expansion that links weak- to strong-coupling behavior in a controlled way. Already the leading order of this expansion was in close agreement with exact results. In the present paper I will present the various details of the calculation not included in the original Letter [16] in a self-contained manner.

The sine-Gordon model is defined by the Hamiltonian

$$H = \int dx \left(\frac{1}{2} \Pi^2(x) + \frac{1}{2} \left(\frac{\partial \phi}{\partial x} \right)^2 + u \tau^{-2} \cos[\beta \phi(x)] \right), \quad (2)$$

where $\phi(x)$ is a bosonic field and $\Pi(x)$ its conjugate momentum field with the commutator $[\Pi(x), \phi(x')] = -i\delta(x - x')$. $u > 0$ is a small dimensionless coupling constant and $\Lambda \propto \tau^{-1}$ an implicit UV-cutoff. We are interested in the universal properties for energies $|E| \ll \Lambda$.

The sine-Gordon model exhibits a strong-coupling phase for $\beta^2 \lesssim 8\pi$ with a mass gap and *fermionic* low-energy excitations (*massive solitons*). The perturbative scaling analysis leads to a characteristic *strong-coupling divergence* of the running coupling u in this regime. This makes the sine-Gordon model an interesting test model for our new approach. The main emphasis in this paper will not lie in deriving new results in this well-studied model, but in showing how these results follow within the flow equation method, and how therefore our new method can be useful for strong-coupling problems more generally.

Other features that make the sine-Gordon model an attractive test model are its interesting phase structure with a Kosterlitz–Thouless type transition to a phase with massless solitons at $\beta^2/8\pi \approx 1 + O(u)$, its integrable structure that allows the comparison with exact results [17,18], and its relation to a variety of other models like the spin-1/2 X–Y–Z chain, the 1d electron gas with backward scattering, the Thirring model in field theory and the 2d Coulomb gas (for an overview of these relations see Ref. [19]). Therefore the results from the flow equation approach can be viewed within a variety of model contexts.

The main motivation for being interested in the flow equation approach to this integrable model lies, however, in the observation that our new method does *not* make use of the integrable structure. In our approach a small parameter is identified and used within a suitably renormalized perturbation expansion. The usual perturbative scaling approach fails because the initially small expansion parameter u diverges during the RG-procedure. In the flow equation approach the expansion parameter will turn out to be the product of the running coupling u and a factor $(-1 + \beta^2/4\pi)$. This combination will *always* remain small during the flow. It is therefore feasible to study for example nonintegrable perturbations and correlation functions within our new approach, which should be of considerable interest in a variety of contexts. Although the calculations presented here appear rather lengthy and technical at first, they are straightforward and much closer to conventional many-body techniques than methods building on the integrable structure.

1.2. Outline

The structure of this paper is as follows. Section 2 deals with some general properties of the sine-Gordon model that are important in the sequel. In Section 2.1 the sine-Gordon model and the regularization used in this paper are introduced. Section 2.2 reviews the perturbative scaling analysis, the phase structure, and the strong-coupling behavior. In Section 2.3 various exact results based on the integrable structure of the sine-Gordon model are summed up, especially properties of the point $\beta^2 = 4\pi$ where the model becomes equivalent to a noninteracting Thirring model. This equivalence will play an important role in understanding the structure of our flow equation approach later on.

After setting the stage in Section 2, Section 3 deals with the actual application of the flow equation approach to the sine-Gordon model. Some general properties of the flow equation method are reviewed in 3.1. Then the appropriate generator $\eta(B)$ for the sine-Gordon model diagonalization is worked out in 3.2 and the commutator $[\eta(B), H_0]$ evaluated in 3.3. The key computational parts of the flow equation approach are contained in 3.4

and 3.5, where the commutators $[\eta(B), H_{\text{int}}(B)]$ and $[\eta(B), H_{\text{diag}}(B)]$ are evaluated. From these commutators the flow of $\beta^2(B)$ and of the running coupling constant are deduced in Section 3.6.

For the convenience of the reader, all the results from this technical part are summed up in Section 4.1, in particular the Hamiltonian $H(B)$ along the flow and the set of flow equations governing the various parameters in $H(B)$. We will see in 4.2 that in the strong-coupling phase $H(B)$ flows to an effective low-energy noninteracting Thirring model. The mass gap of the sine-Gordon model can be easily deduced from this low-energy model, and the results are then compared with perturbative scaling analysis and exact integrable model results. The agreement will turn out to be very good. In Section 4.3 the final diagonal Hamiltonian $H(B = \infty)$ is discussed in more detail, in particular the soliton dispersion relation and properties in the crossover region. Finally in Section 4.4 the approximations and the expansion parameter of our approach are reviewed.

Section 5 sums up the conclusions and an outlook to open questions. The appendix contains important properties of vertex operators that are used throughout this paper.

2. Sine-Gordon model

2.1. Definition

The one-dimensional quantum sine-Gordon model is defined by the Hamiltonian

$$H = \int dx \left(\frac{1}{2} \Pi^2(x) + \frac{1}{2} \left(\frac{\partial \phi}{\partial x} \right)^2 + u \tau^{-2} \cos[\beta \phi(x)] \right). \quad (3)$$

$\phi(x)$ is a bosonic field and $\Pi(x)$ its conjugate momentum field with the fundamental commutator

$$[\Pi(x), \phi(x')] = -i \delta(x - x'). \quad (4)$$

In (3) an UV-momentum cutoff $\Lambda \propto \tau^{-1}$ is implied. u is a dimensionless coupling constant. Without loss of generality we will assume $u > 0$ and $\beta > 0$.

Expanding the fields in normal modes gives

$$\phi(x) = -\frac{i}{\sqrt{4\pi}} \sum_{k \neq 0} \frac{\sqrt{|k|}}{k} e^{-ikx} (\sigma_1(k) + \sigma_2(k)), \quad (5)$$

$$\Pi(x) = \frac{1}{\sqrt{4\pi}} \sum_{k \neq 0} \sqrt{|k|} e^{-ikx} (\sigma_1(k) - \sigma_2(k)). \quad (6)$$

Sums over wavevectors k, p, q, \dots are to be understood in the sense

$$\sum_k \stackrel{\text{def}}{=} \frac{2\pi}{L} \sum_{n=-\infty}^{\infty} \quad (7)$$

with $k = 2\pi n/L$ throughout this paper. L is the system size. The basic commutators for $k, k' > 0$ are

$$\begin{aligned} [\sigma_1(-k), \sigma_1(k')] &= [\sigma_2(k), \sigma_2(-k')] = \delta_{kk'} L/2\pi, \\ [\sigma_j(k), \sigma_j(k')] &= [\sigma_j(-k), \sigma_j(-k')] = 0 \end{aligned} \tag{8}$$

and for $j \neq j'$

$$[\sigma_j(k), \sigma_{j'}(k')] = [\sigma_j(-k), \sigma_{j'}(k')] = [\sigma_j(-k), \sigma_{j'}(-k')] = 0. \tag{9}$$

All other commutators can be derived via $\sigma_i^\dagger(-k) = \sigma_i(k)$. The vacuum $|\Omega\rangle$ is defined by

$$\sigma_1(-k)|\Omega\rangle = \sigma_2(k)|\Omega\rangle = 0 \tag{10}$$

for all $k > 0$. The notion of the *dual field* $\Theta(x)$ will also be useful. $\Theta(x)$ is defined by

$$\partial_x \Theta(x) = -\Pi(x), \tag{11}$$

leading to the commutator

$$[\Theta(x), \phi(x')] = i\theta(x - x'). \tag{12}$$

In terms of normal modes one finds

$$\Theta(x) = -\frac{i}{\sqrt{4\pi}} \sum_{k \neq 0} \frac{\sqrt{|k|}}{k} e^{-ikx} (\sigma_1(k) - \sigma_2(k)). \tag{13}$$

The concept of *vertex operators* will play an important role in the sequel. Vertex operators $V_j(\alpha; x)$ are defined as normal-ordered exponentials

$$V_j(\alpha; x) = : \exp\left(\pm\alpha \sum_{p \neq 0} \frac{\sqrt{|p|}}{p} e^{-\frac{a}{2}|p|-ipx} \sigma_j(p)\right) : \tag{14}$$

with + (upper sign) corresponding to $j = 1$ and – (lower sign) to $j = 2$. This sign convention will be used throughout this paper. Normal ordering $: \dots :$ amounts to commuting all the operators that annihilate the vacuum according to (10) to the right. One can rewrite (14) in terms of the field and its dual (11)

$$V_j(\alpha; x) = : \exp\left(\pm i\alpha \sqrt{\pi} \int d\epsilon c(\epsilon) [\phi(x + \epsilon) \pm \Theta(x + \epsilon)]\right) : \tag{15}$$

with the Lorentzian

$$c(\epsilon) = \frac{a/2\pi}{\epsilon^2 + a^2/4}. \tag{16}$$

$c(\epsilon)$ is normalized

$$\int_{-\infty}^{\infty} d\epsilon c(\epsilon) = 1 \tag{17}$$

and $c(\epsilon) \xrightarrow{a \rightarrow 0} \delta(\epsilon)$. Further properties of vertex operators, in particular their operator product expansion (OPE), are reviewed in Appendix A.

One can rewrite the interaction term of the sine-Gordon model (3) in terms of vertex operators

$$H = \int dx \left(\frac{1}{2} \Pi^2(x) + \frac{1}{2} \left(\frac{\partial \phi}{\partial x} \right)^2 + \frac{u}{2\pi a^2} \left(\frac{2\pi a}{L} \right)^{\alpha^2} (V_1(\alpha; x) V_2(-\alpha; x) + V_2(\alpha; x) V_1(-\alpha; x)) \right). \quad (18)$$

The prefactor $(2\pi a/L)^{\alpha^2}$ follows from (A6). Here and in the sequel α and β are used interchangeably with the identification

$$\alpha \stackrel{\text{def}}{=} \frac{\beta}{\sqrt{4\pi}}. \quad (19)$$

Eq. (18) is the form of the sine-Gordon Hamiltonian that we will investigate with the flow equation approach. No implicit momentum cutoff is implied in (18): the UV-regularization of the Hamiltonian (18) is achieved by the cutoff parameter $a > 0$ in the vertex operators. The regularizations in (18) and (3) are related by $a^{-1} \propto \Lambda \propto \tau^{-1}$. For a direct comparison between the original Hamiltonian (3) and the form (18) used here one can also identically express (18) as

$$H = \int dx \left(\frac{1}{2} \Pi^2(x) + \frac{1}{2} \left(\frac{\partial \phi}{\partial x} \right)^2 + \frac{u}{\pi a^2} \cos \left[\beta \int d\epsilon c(\epsilon) \phi(x + \epsilon) \right] \right). \quad (20)$$

The regularization with a therefore amounts to *smearing out* the interaction term. In the limit $a \rightarrow 0$ one recovers the $\cos(\beta\phi(x))$ -interaction term.

The universal properties of the sine-Gordon model for energies $|E| \ll a^{-1}$ are not affected by this choice of regularization. We find, however, notational simplifications and more compact expressions in the course of our calculation when we start with (18) (or equivalently (20)). In order to clarify the main conceptual ideas of the flow equation approach, it will therefore be convenient for us to use the regularization (18) with the UV-cutoff a^{-1} built in via the definition of the vertex operators.

2.2. Perturbative scaling analysis

The flow equation approach can be viewed as an extension of perturbative scaling. Therefore it is useful to briefly review the results of the perturbative scaling analysis as applied to the sine-Gordon model. A comprehensive review can be found in Ref. [20].

In 2-loop order there are two renormalization group equations that describe the flow of u and β upon integrating out the degrees of freedom with $\Lambda - d\Lambda < |k| < \Lambda$ (see Ref. [21])

$$\frac{d\beta^{-2}}{d \ln \Lambda} = -\frac{u^2}{4\pi}, \quad \frac{du}{d \ln \Lambda} = \left(\frac{\beta^2}{4\pi} - 2 \right) u. \quad (21)$$

The initial conditions are $u(\tau^{-1}) = u$ and $\beta(\tau^{-1}) = \beta$. These scaling equations give rise to the Kosterlitz–Thouless type phase diagram shown in Fig. 1. The two separatrices S_{\pm} originating from $\beta^2 = 8\pi$ with $\beta^2 = 8\pi(1 \pm u)$ for small u divide the parameter space in three sectors:

1. The weak-coupling sector I;
2. The crossover sector II;

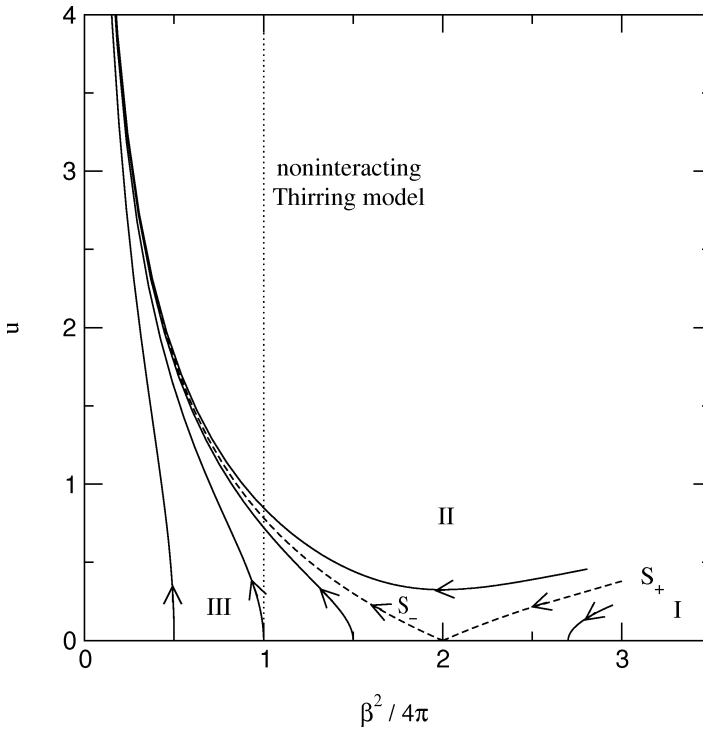


Fig. 1. Perturbative scaling flow and the phase diagram of the sine-Gordon model. The strong-coupling phase is to the left and/or above the KT-transition line S_+ (dashed line for $\beta^2 \geq 8\pi$), the weak-coupling phase below S_+ . $\beta^2 = 4\pi$ (dotted line) corresponds to the noninteracting Thirring model, see Section 2.3.

3. The asymptotic freedom sector III.

Both in II and III the perturbative scaling equations (21) lead to *strong-coupling* behavior with the running coupling constant u growing larger and larger during the flow. Therefore the perturbative RG approach eventually becomes invalid in these sectors. This indicates the opening of mass gap in the spectrum in II and III. Across S_+ the system undergoes a Kosterlitz–Thouless type phase transition between this massive phase and the massless phase in I.

In spite of the strong-coupling divergence in II and III, the perturbative scaling equations allow us to analyze the size of the mass gap by identifying the mass M with the scaling invariant of (21). One, e.g., finds the following expressions for small $u > 0$

$$M \propto \Lambda \left(\frac{u}{2 - \beta^2/4\pi} \right)^{1/(2 - \beta^2/4\pi)} \quad \text{for } \frac{1 - \beta^2/8\pi}{u} \gg 1, \quad (22)$$

$$M \propto \Lambda \exp\left(-\frac{1}{2 - \beta^2/4\pi}\right) \quad \text{for } \left(1 - \frac{\beta^2}{8\pi} - u\right)^{-1} \gg 1 \quad (\text{along } S_-), \quad (23)$$

$$M \propto \Lambda \exp\left(-\frac{\pi}{2\sqrt{u^2 - (1 - \beta^2/8\pi)^2}}\right) \quad \text{for } \left(1 - \frac{\beta^2}{8\pi} + u\right)^{-1} \gg 1 \quad (\text{along } S_+). \quad (24)$$

In this manner one can obtain information about the renormalized low-energy scale even in the strong-coupling phase. But the perturbative scaling approach does by itself not lead to an understanding of the physical behavior associated with this low-energy scale. This situation is typical for other strong-coupling problems as well, the Kondo model being the paradigm in condensed matter theory [1]. In combination with mappings to other exactly solvable models these shortcomings can sometimes be partially overcome, see Section 2.3 below. However, in general there is considerable interest in theoretical methods that can solve strong-coupling problems in a controlled way. Therefore the flow equation approach might be an interesting tool also for other strong-coupling problems by removing some of the above shortcomings.

The phase diagram Fig. 1 remains essentially unchanged in higher loop orders [20]. For latter comparison with the flow equation solution it is interesting to also write down the 3-loop result for the mass gap on S_- (that is for $\beta^2 = 8\pi(1-u)$) in the limit $u \rightarrow 0$

$$M \propto \Lambda u^{1/2} \exp\left(-\frac{1}{2u}\right). \quad (25)$$

Notice the $u^{1/2}$ -prefactor as compared to the 2-loop result (23). Higher loop orders beyond 3-loop should only affect the proportionality factor in (25) [20].

2.3. Integrable structure and relation to other models

The sine-Gordon model is one of the best studied integrable models, which makes it a very suitable test model for our new approach. Its spectrum was obtained exactly from an inverse scattering solution [17] and its S -matrix was calculated by Zamolodchikov [18]. For a recent review see Ref. [22].

In the strong-coupling phase the exact solution confirms the scaling behavior (22) for the mass M of the solitons and antisolitons. The exact S -matrix [18] also shows that for small rapidity differences these solitons and antisolitons behave as fermions. This important observation of a *change in statistics* for the low-energy excitations will be reproduced in our flow equation framework.

In addition, the exact solution shows that new features appear for $\beta^2 < 4\pi$: soliton–antisoliton bound states (*breathers*) emerge in the spectrum with excitation energies smaller than $2M$. There is one breather for $8\pi/3 \leq \beta^2 < 4\pi$, two breathers for $2\pi \leq \beta^2 < 8\pi/3$, etc. [22].

The sine-Gordon model is related to other integrable models like the spin-1/2 X–Y–Z chain and the Thirring model. Since in particular the relation to the Thirring model will be fruitful in the sequel, it is useful to sum up some of its main properties here: The massive 1d Thirring model is defined by the Lagrangian density

$$\mathcal{L}_{\text{Th}} = \sum_{\mu=0}^1 \left(\bar{\psi} i \gamma_{\mu} \partial^{\mu} \psi - \frac{1}{2} g j_{\mu} j^{\mu} \right) - M \bar{\psi} \psi \quad (26)$$

in terms of the two-component spinor $\psi(x)$

$$\psi(x) = \begin{pmatrix} \psi_1(x) \\ \psi_2(x) \end{pmatrix} \tag{27}$$

with components obeying fermionic anticommutation relations

$$\{\psi_j(x), \psi_{j'}^\dagger(y)\} = \delta_{jj'}\delta(x - y), \quad \{\psi_j(x), \psi_{j'}(y)\} = \{\psi_j^\dagger(x), \psi_{j'}^\dagger(y)\} = 0. \tag{28}$$

The current is defined by $j^\mu \stackrel{\text{def}}{=} \bar{\psi} \gamma^\mu \psi$ with $\bar{\psi} \stackrel{\text{def}}{=} \psi^\dagger \gamma_0$ and the γ -matrices are explicitly given by

$$\gamma_0 = \begin{pmatrix} 0 & 1 \\ 1 & 0 \end{pmatrix} \quad \text{and} \quad \gamma_1 = \begin{pmatrix} 0 & 1 \\ -1 & 0 \end{pmatrix}. \tag{29}$$

The exact Bethe ansatz solution of the Thirring model was obtained by Bergknoff and Thacker [23].

Coleman [24] has shown the equivalence of the sine-Gordon model with the Thirring model (26) order by order in perturbation theory with the following mapping between the coupling constants

$$\frac{\beta^2}{4\pi} = \frac{1}{1 + g/\pi}. \tag{30}$$

One notices that $\beta^2 = 4\pi$ is a special point of the sine-Gordon model since it corresponds to a *noninteracting* massive Thirring model ($g = 0$). For $\beta^2 = 4\pi$ the elementary excitations of the sine-Gordon model are therefore *fermionic* with the dispersion relation $\pm E_k$ with

$$E_k = \sqrt{k^2 + M^2}. \tag{31}$$

The explicit relation between the bosonic field of the sine-Gordon model and the fermionic field of the Thirring model was found by Mandelstam [25]. For $\beta^2 = 4\pi$ one has explicitly

$$\psi_j(x) = \frac{1}{\sqrt{L}} V_j(-1; x) \tag{32}$$

with $V_j(\alpha; x)$ from (14) (notice that the $V_j(\pm 1; x)$ obey anticommutation relations (A20) in the limit $a \rightarrow 0$). These *Thirring fermions*¹ correspond to the quantized soliton solutions of the sine-Gordon model [25].

The perturbative scaling approach does not “know” about the special point $\beta^2 = 4\pi$ where the sine-Gordon model is trivially diagonalizable by using the equivalence to the quadratic Thirring model: the strong-coupling scaling trajectories in Fig. 1 go right through the line $\beta^2 = 4\pi$. The subsequent strong-coupling divergence of the running coupling constant is then due to the fact that one has generated the nonvanishing energy scale M . A similar scenario occurs in the Kondo model: there the diagonal Hamiltonian corresponds to the Toulouse point [26] and the nonvanishing energy scale is the Kondo temperature T_K .

¹ Notice, however, that $V_1(\pm 1; x)$ commutes with $V_2(\pm 1; x)$ instead of anticommuting. “Proper” fermions can easily be defined with an additional Jordan–Wigner phase factor, but nothing new can be learned from this Jordan–Wigner construction.

A standard approach to avoid the strong-coupling divergence is to scale the model to the exactly solvable line $\beta^2 = 4\pi$: one stops the scaling once $\beta^2(\Lambda_{\text{eff}}) = 4\pi$ and obtains the mass from the value of the running coupling constant. With this approach it is also plausible that the low-energy single-particle/hole excitations in the strong-coupling phase are fermionic with a mass set by the scaling invariant. Though very useful, this is an uncontrolled approximation since the running coupling constant is already large when $\beta^2(\Lambda_{\text{eff}}) = 4\pi$. It is therefore difficult/impossible to learn something about the crossover from weak-coupling to strong-coupling or about the effect of irrelevant operators at the strong-coupling fixed point. These shortcomings make it desirable to develop our new method that will allow a systematic expansion describing the full crossover flow.

The sine-Gordon model is also related to a variety of other models like the 2d Coulomb gas with temperature $T = \beta^{-2}$ and fugacity $z \propto u$, or a 1d electron gas with backward scattering. For an overview of these and other relations see Ref. [19]. As a final remark we also want to mention that the mapping to the 1d electron gas gives a natural interpretation to the separatrices S_{\pm} in Fig. 1 since they correspond to an electron gas with SU(2) spin-symmetric interactions [19]. The sine-Gordon model with $\beta^2 = 8\pi(1 \pm u)$, $|u| \ll 1$ therefore carries a hidden SU(2)-symmetry.

3. Flow equation approach

3.1. General concepts

The idea to apply a sequence of infinitesimal unitary transformations to a Hamiltonian in order to make it more diagonal has been independently put forward by Wegner [2] and Głazek and Wilson [3,4]. Wegner's original work focussed on diagonalizing many-particle Hamiltonians, whereas the focus in the work of Głazek and Wilson was to construct effective low-energy Hamiltonians for strong-coupling field theories: such effective Hamiltonians can then be analyzed by standard techniques in order to find the bound state spectrum, which in turn could be interpreted as, e.g., hadrons or mesons. Though the outlook of these approaches is somehow different, the concepts are very similar. In this paper we will follow Wegner's methodology.

The main idea of Wegner's *flow equations* is to generate a one-parameter family of unitarily equivalent Hamiltonians $H(B)$ labelled by a *flow parameter* B .² This is achieved by solving a differential equation

$$\frac{dH(B)}{dB} = [\eta(B), H(B)] \quad (33)$$

with some anti-Hermitian generator $\eta(B) = -\eta^\dagger(B)$ where $H(B=0) = H$ is the initial Hamiltonian. One wants to choose $\eta(B)$ such that $H(B)$ becomes more diagonal as $B \rightarrow \infty$: splitting up $H(B)$ in its diagonal and interaction parts

² The flow parameter has been denoted by ℓ in most other works on flow equations. In order to avoid confusion with the common notation where ℓ is the logarithm of the change in length scale in RG-equations, B instead of ℓ is used in this work.

$$H(B) = H_0(B) + H_{\text{int}}(B), \quad (34)$$

this amounts to requiring $H_{\text{int}}(B)$ becomes (in some sense) smaller for $B \rightarrow \infty$. In order to achieve this, Wegner proposed the following generator [2]

$$\eta(B) \stackrel{\text{def}}{=} [H_0(B), H_{\text{int}}(B)]. \quad (35)$$

With this choice of $\eta(B)$ one can show

$$\frac{d}{dB} \text{Tr} H_{\text{int}}^2(B) \leq 0 \quad (36)$$

and in this sense the operator $H_{\text{int}}(B)$ becomes smaller along the flow. Notice that B has the dimension of $(\text{Energy})^{-2}$ with this choice. However, for a many-particle Hamiltonian Eq. (36) is usually not well-defined since the trace is typically infinite. Also higher and higher order interactions are successively generated by the system of Eqs. (33) and (35), which have to be truncated in some way making rigorous statements difficult.

Still one finds that (35) is generally a suitable choice for achieving our goal to make the initial Hamiltonian diagonal if $H_{\text{int}}(B=0)$ can be viewed as a small perturbation term: truncating the system of higher order interactions produced by (33) and (35) in some order of the coupling constant then amounts to generating a perturbation expansion in a renormalized coupling constant. From this point of view the flow equation approach is similar to perturbative RG. Matrix elements of $H_{\text{int}}(B=0)$ that couple states with large energy differences are eliminated in the initial stages of the flow (for small B), and matrix elements coupling more degenerate states are eliminated later. This is reminiscent of the energy scale separation underlying the renormalization group approach, which is the suitable perturbation expansion for systems with largely varying energy scales.

Explicit applications of these ideas have been discussed for various model Hamiltonians like the n -orbital model [2,5], dissipative quantum systems [6,7], systems with electron–phonon coupling [9–11] and various other models in condensed matter physics [8,12,13,15,27,28]. In the present paper it will be shown how this method can be used for the sine-Gordon model as a genuine strong-coupling many-body Hamiltonian.

3.2. Generator η

The aim of this work is to diagonalize the sine-Gordon model (18) using the method of infinitesimal unitary transformations outlined above. We split up the sine-Gordon Hamiltonian $H(B)$ into a free part H_0 and the interaction part $H_{\text{int}}(B)$

$$H(B) = H_0 + H_{\text{int}}(B) \quad (37)$$

with

$$H_0 = \int dx \left(\frac{1}{2} \Pi^2(x) + \frac{1}{2} \left(\frac{\partial \phi}{\partial x} \right)^2 \right) = \sum_{p>0} p (\sigma_1(p) \sigma_1(-p) + \sigma_2(-p) \sigma_2(p)), \quad (38)$$

$$H_{\text{int}}(B) = \int dx dy u(B; y) (V_1(\alpha; x) V_2(-\alpha; x-y) + \text{h.c.}). \quad (39)$$

In order to avoid confusion the initial parameters u and β in (18) will from now on be denoted as u_0 and β_0 . The initial condition for (39) then reads

$$\alpha = \frac{\beta_0}{\sqrt{4\pi}}, \quad u(B = 0; y) = \frac{u_0}{2\pi a^2} \delta(y) \left(\frac{2\pi a}{L}\right)^{\alpha^2}. \tag{40}$$

Notice that we have already allowed for a general nonlocal interaction $u(B; y)$ in (39) since the initially local interaction (40) will become nonlocal along the flow (see below). Next we have to evaluate (35). The following commutator is useful

$$[\sigma_j(p), V_{j'}(\alpha; x)] = \delta_{jj'} \alpha \frac{\sqrt{|p|}}{p} \exp\left(-\frac{a}{2}|p| + ipx\right) V_{j'}(\alpha; x) \tag{41}$$

leading to

$$\begin{aligned} \left[\sum_{p>0} p \sigma_1(p) \sigma_1(-p), V_1(\alpha; x) \right] &= i \partial_x V_1(\alpha; x), \\ \left[\sum_{p>0} p \sigma_2(-p) \sigma_2(p), V_2(\alpha; x) \right] &= -i \partial_x V_2(\alpha; x). \end{aligned} \tag{42}$$

Thus we find the following generator

$$\begin{aligned} \eta(B) &= [H_0, H_{\text{int}}(B)] \\ &= -2i \int dx dy \frac{\partial u(B; y)}{\partial y} (V_1(\alpha; x) V_2(-\alpha; x - y) + \text{h.c.}). \end{aligned} \tag{43}$$

3.3. Commutator $[\eta, H_0]$

To study the flow generated by η we first look at the commutator $[\eta, H_0]$. Using (42) one easily shows

$$[\eta, H_0] = 4 \int dx dy \frac{\partial^2 u(B; y)}{\partial y^2} (V_1(\alpha; x) V_2(-\alpha; x - y) + \text{h.c.}). \tag{44}$$

Comparison of the coefficients on the left-hand side of (33) with (44) gives

$$\frac{\partial u(B; y)}{\partial B} = 4 \frac{\partial^2 u(B; y)}{\partial y^2}, \tag{45}$$

where possible contributions from $[\eta, H_{\text{int}}]$ are still missing. Eq. (45) has the character of a diffusion equation: the initially local interaction becomes increasingly non-local along the flow. In terms of Fourier coefficients

$$u(B; y) = \sum_p u(B; p) e^{-ipy} \tag{46}$$

one finds the solution

$$u(B; p) = \frac{u_0}{4\pi^2 a^2} e^{-4p^2 B} \left(\frac{2\pi a}{L}\right)^{\alpha^2}. \tag{47}$$

One sees explicitly that matrix elements $u(B; p)$ coupling states with large energy differences $|p|$ are eliminated in the early stages of the flow (for small B), whereas matrix elements coupling more degenerate states are decoupled later during the flow. This is a generic feature of Wegner’s generator (35).

Later we will see that (47) is modified due to higher-order contributions. Therefore we introduce a more general parametrization

$$u(B; p) = \frac{\tilde{u}(B)}{4\pi^2 a^2} \left(\frac{2\pi a}{L} \right)^{\alpha^2(B)} v(B; p) \tag{48}$$

with a *running coupling* $\tilde{u}(B)$, initially $\tilde{u}(B = 0) = u_0$. The differential equation for the coefficients $v(B; p)$ now reads

$$\frac{\partial v(B; p)}{\partial B} = -4p^2 v(B; p) \tag{49}$$

with the initial condition $v(B = 0; p) = 1$.

3.4. Commutator $[\eta, H_{\text{int}}]$

3.4.1. General properties

The evaluation of $[\eta, H_{\text{int}}]$ is the key calculation in the flow equation approach. We first look at some general properties of such commutators. Let A_1, A_2, B_1, B_2 be arbitrary operators with $[A_j, B_{j'}] = 0$. We define $*O*$ as the operator with its ground state expectation value subtracted

$$*O* \stackrel{\text{def}}{=} O - \langle O \rangle, \tag{50}$$

with the notation $\langle O \rangle \stackrel{\text{def}}{=} \langle \Omega | O | \Omega \rangle$. One easily shows

$$\begin{aligned} [A_1 B_1, A_2 B_2] &= \langle A_1 A_2 \rangle \langle B_1 B_2 \rangle - \langle A_2 A_1 \rangle \langle B_2 B_1 \rangle + \langle B_1 B_2 \rangle * A_1 A_2 * \\ &\quad - \langle B_2 B_1 \rangle * A_2 A_1 * + \langle A_1 A_2 \rangle * B_1 B_2 * \\ &\quad - \langle A_2 A_1 \rangle * B_2 B_1 * + R \end{aligned} \tag{51}$$

with

$$R = *A_1 A_2 * *B_1 B_2 * - *A_2 A_1 * *B_2 B_1 * . \tag{52}$$

In general R leads to the generation of higher-order interaction terms during the flow. R vanishes if the operators fulfill the following exchange relations

$$A_1 A_2 + e^{i\phi} A_2 A_1 = c, \quad B_1 B_2 + e^{-i\phi} B_2 B_1 = c \tag{53}$$

with fixed ϕ and c . E.g., for $\phi = 0$ these are fermionic anticommutation relations, or for $\phi = \pi$ bosonic commutation relations. Then no higher-order interactions are generated and it is possible to close the flow equations without approximations. For general β_0 in the interaction term we will, however, have to develop a suitable approximation for R in the next section.

3.4.2. $[\eta, H_{\text{int}}]$ in the sine-Gordon model

There are two structurally different commutators of vertex operators generated by $[\eta, H_{\text{int}}]$ in the sine-Gordon model: $[V_1 V_2^\dagger, V_1^\dagger V_2]$ and $[V_1 V_2^\dagger, V_1 V_2^\dagger]$ (or equivalently $[V_1^\dagger V_2, V_1^\dagger V_2]$). The first term

$$[V_1(\alpha; x_1)V_2(-\alpha; x_1 - y_1), V_1(-\alpha; x_2)V_2(\alpha; x_2 - y_2)] \tag{54}$$

and its hermitian conjugate will turn out to be the leading contributions and are discussed first. Eqs. (A16) and (A17) give

$$\begin{aligned} \langle V_1(\alpha; x_1)V_1(-\alpha; x_2) \rangle &= s_1^{-\alpha^2}, & \langle V_1(-\alpha; x_2)V_1(\alpha; x_1) \rangle &= \bar{s}_1^{-\alpha^2}, \\ \langle V_2(-\alpha; x_1 - y_1)V_2(\alpha; x_2 - y_2) \rangle &= s_2^{-\alpha^2}, \\ \langle V_2(\alpha; x_2 - y_2)V_2(-\alpha; x_1 - y_1) \rangle &= \bar{s}_2^{-\alpha^2} \end{aligned} \tag{55}$$

with

$$s_1 = \frac{2\pi}{L}(i(x_2 - x_1) + a), \quad s_2 = \frac{2\pi}{L}(i(x_1 - y_1 - x_2 + y_2) + a). \tag{56}$$

Using (51) we then find

$$\begin{aligned} &[V_1(\alpha; x_1)V_2(-\alpha; x_1 - y_1), V_1(-\alpha; x_2)V_2(\alpha; x_2 - y_2)] \\ &= s_1^{-\alpha^2} s_2^{-\alpha^2} - \bar{s}_1^{-\alpha^2} \bar{s}_2^{-\alpha^2} \\ &\quad + s_2^{-\alpha^2} * V_1(\alpha; x_1)V_1(-\alpha; x_2) * - \bar{s}_2^{-\alpha^2} * V_1(-\alpha; x_2)V_1(\alpha; x_1) * \\ &\quad + s_1^{-\alpha^2} * V_2(-\alpha; x_1 - y_1)V_2(\alpha; x_2 - y_2) * \\ &\quad - \bar{s}_1^{-\alpha^2} * V_2(\alpha; x_2 - y_2)V_2(-\alpha; x_1 - y_1) * + R \end{aligned} \tag{57}$$

with

$$\begin{aligned} R &= *V_1(\alpha; x_1)V_1(-\alpha; x_2) * *V_2(-\alpha; x_1 - y_1)V_2(\alpha; x_2 - y_2) * \\ &\quad - *V_1(-\alpha; x_2)V_1(\alpha; x_1) * *V_2(\alpha; x_2 - y_2)V_2(-\alpha; x_1 - y_1) *. \end{aligned} \tag{58}$$

The key approximation in our method is to use an operator product expansion (OPE) in higher-order interaction terms like R , and then to neglect contributions with larger scaling dimensions (more irrelevant terms in the RG-sense). From (A18) we, e.g., conclude

$$\begin{aligned} &*V_1(\alpha; x_1)V_1(-\alpha; x_2) * \\ &= s_1^{-\alpha^2} \left(i\alpha(x_2 - x_1) \sum_{p \neq 0} \sqrt{|p|} e^{-\frac{a}{2}|p| - ipx_1} \sigma_1(p) + \dots \right), \end{aligned} \tag{59}$$

where we have neglected the higher-order terms in (A18). Notice that the c -number contribution has already been removed by subtracting the ground state expectation value. Putting everything together gives

$$\begin{aligned} R &= \alpha^2(x_2 - x_1)(x_1 - y_1 - x_2 + y_2) (s_1^{-\alpha^2} s_2^{-\alpha^2} - \bar{s}_1^{-\alpha^2} \bar{s}_2^{-\alpha^2}) \\ &\quad \times \sum_{p, q \neq 0} \sqrt{|p q|} e^{-\frac{a}{2}(|p| + |q|) - ipx_1 - iq(x_1 - y_1)} \sigma_1(p) \sigma_2(q). \end{aligned} \tag{60}$$

The first and second term in (57) are c -numbers and describe a shift in the ground state energy. This is of no particular interest and we will not look into it. The various other terms generated in $[\eta, H_{\text{int}}]$ are discussed in the next subsections.

3.4.3. R -term

The R -term in (57) leads to the following contribution from $[\eta, H_{\text{int}}]$

$$\begin{aligned}
 & -2i \int dx_1 dx_2 dy_1 dy_2 \frac{\partial u(B; y_1)}{\partial y_1} u(B; y_2) 2\alpha^2 (x_2 - x_1)(x_1 - y_1 - x_2 + y_2) \\
 & \times (s_1^{-\alpha^2} s_2^{-\alpha^2} - \bar{s}_1^{-\alpha^2} \bar{s}_2^{-\alpha^2}) \sum_{p, q \neq 0} \sqrt{|p q|} e^{-\frac{a}{2}(|p|+|q|) - ipx_1 - iq(x_1 - y_1)} \sigma_1(p) \sigma_2(q) \\
 & = -8\pi i \alpha^2 \left(\frac{L}{2\pi}\right)^{2\alpha^2} \sum_{k \neq 0} |k| t_k \sigma_1(k) \sigma_2(-k)
 \end{aligned} \tag{61}$$

with coefficients t_k

$$\begin{aligned}
 t_k & = \int dz_1 dz_2 dz_3 e^{-a|k| - ikz_1} \frac{\partial u(B; z_1)}{\partial z_1} u(B; z_1 + z_2) z_3 (z_2 - z_3) \\
 & \times ((iz_3 + a)^{-\alpha^2} (iz_2 - z_3 + a)^{-\alpha^2} - \text{h.c.}).
 \end{aligned} \tag{62}$$

Except for an (unimportant) initial transient where $B \lesssim a^2$, the z_1 -integral leads to the following expression:

$$t_k = -2\pi i a^{4-2\alpha^2} \sum_p p u(B; p) u(B; -k - p) \int dx e^{i(k+p)ax} I(x) \tag{63}$$

with

$$\begin{aligned}
 I(x) & = \int dy y(x - y) \\
 & \times ((1 + iy)^{-\alpha^2} (1 - iy + ix)^{-\alpha^2} - (1 - iy)^{-\alpha^2} (1 + iy - ix)^{-\alpha^2}).
 \end{aligned} \tag{64}$$

Writing $1 + i(y \pm \frac{x}{2}) = r_{\pm} e^{i\phi_{\pm}}$ with

$$r_{\pm} = \sqrt{1 + \left(y \pm \frac{x}{2}\right)^2}, \quad \phi_{\pm} = \arcsin \frac{y \pm \frac{x}{2}}{r_{\pm}} \in \left[-\frac{\pi}{2}, \frac{\pi}{2}\right] \tag{65}$$

leads to

$$I(x) = 2i \int dy \left(\frac{x^2}{4} - y^2\right) (r_+ r_-)^{-\alpha^2} \sin(\alpha^2(\phi_- - \phi_+)). \tag{66}$$

The flow is dominated by the term decaying most slowly with B , which corresponds to the large- x behavior of $I(x)$. Therefore we can approximate

$$r_{\pm} \approx \left|\frac{x}{2}\right| |z \pm 1|, \tag{67}$$

where $z = 2y/x$, and find

$$I(x) = 2i \left| \frac{x}{2} \right|^{3-2\alpha^2} \int_{-\infty}^{\infty} dz (1-z^2) |1-z^2|^{-\alpha^2} \sin(\alpha^2(\phi_- - \phi_+)). \tag{68}$$

With the above approximation one has $\phi_{\pm} \in \{-\frac{\pi}{2}, \frac{\pi}{2}\}$. Thus the only contributions to $I(x)$ come from regions with $\phi_- \neq \phi_+$

$$\begin{aligned} \phi_- - \phi_+ = -\pi &\Rightarrow x > 0, \quad -1 < z < 1, \\ \phi_- - \phi_+ = \pi &\Rightarrow x < 0, \quad -1 < z < 1 \end{aligned} \tag{69}$$

leading to

$$\begin{aligned} I(x) &= -2i \sin(\alpha^2\pi) \operatorname{sgn}(x) \left| \frac{x}{2} \right|^{3-2\alpha^2} \int_{-1}^1 dz (1-z^2)^{1-\alpha^2} \\ &= 2i \frac{\pi^{3/2}}{\Gamma(\alpha^2-1) \Gamma(\frac{5}{2}-\alpha^2)} \operatorname{sgn}(x) \left| \frac{x}{2} \right|^{3-2\alpha^2}. \end{aligned} \tag{70}$$

With (48) and (49) the sum over p in (63) gives

$$\begin{aligned} &\sum_p p u(B; p) u(B; -k-p) e^{ipax} \\ &= i \left(\frac{\tilde{u}(B)}{4\pi^2 a^2} \right)^2 \left(\frac{2\pi a}{L} \right)^{2\alpha^2} \sqrt{\frac{\pi}{8B}} \left(\frac{ax}{16B} + \frac{ik}{2} \right) \exp\left(-\frac{a^2 x^2}{32B} - \frac{ikax}{2} - 2Bk^2 \right). \end{aligned} \tag{71}$$

The final step is to perform the x -integration in (63). This can be done in closed form leading to hypergeometric functions. However, the flow is determined by the IR-limit $k \rightarrow 0$ where the integral is simpler

$$t_{k=0} = i \frac{32\pi^3}{\Gamma(\alpha^2-1)} (32B)^{1-\alpha^2} \left(\frac{\tilde{u}(B)}{4\pi^2 a^2} \right)^2 \left(\frac{2\pi a}{L} \right)^{2\alpha^2}. \tag{72}$$

For the full k -dependence we write

$$t_k = t_{k=0} f(\alpha^2; k\sqrt{B}). \tag{73}$$

To leading order the only information that we will need about $f(\alpha^2; x)$ is that it falls off rapidly to zero for large arguments $|x| \gg 1$. For example one easily shows

$$\begin{aligned} f(\alpha^2 = 1; x) &= e^{-4x^2} (1 - 8x^2), \\ f(\alpha^2 = 2; x) &= e^{-4x^2} - \sqrt{2\pi} x \operatorname{erf}(\sqrt{2}x) e^{-2x^2}. \end{aligned} \tag{74}$$

These functions are depicted in Fig. 2.

Putting everything together the R -terms in (57) from $[\eta, H_{\text{int}}]$ contribute

$$[\eta, H_{\text{int}}] \longrightarrow \frac{32}{a^2} \left(\frac{32B}{a^2} \right)^{1-\alpha^2} \frac{\alpha^2}{2\Gamma(\alpha^2-1)} \tilde{u}^2(B) \sum_{k \neq 0} |k| f(\alpha^2; k\sqrt{B}) \sigma_1(k) \sigma_2(-k). \tag{75}$$

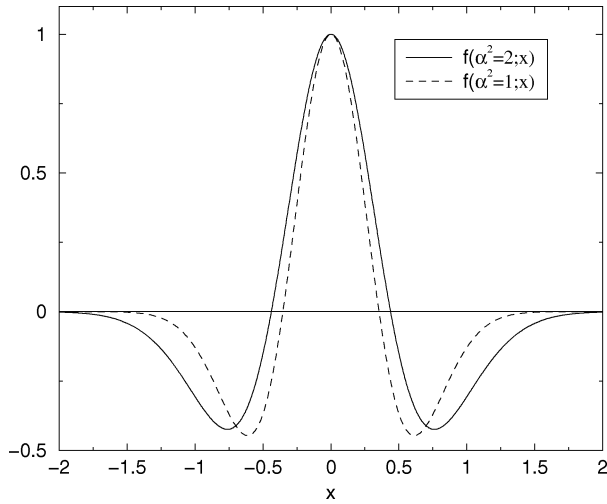


Fig. 2. $f(\alpha^2; x)$ for $\alpha^2 = 2$ and $\alpha^2 = 1$, see Eq. (74).

An important observation can be made for $\alpha = 1$: due to the divergent Γ -function in the denominator, the term (75) vanishes for $\beta_0^2 = 4\pi$. This is an immediate consequence of the fact that in this case the vertex operators describe fermions. The interaction term of the sine-Gordon model is then simply a quadratic term in the fermions and no higher-order interactions are generated during the flow, therefore according to (53) $R \equiv 0$ for all B . For $\beta_0^2 = 4\pi$ we will be able to solve the flow equations without any approximations, thereby recovering the equivalence to the noninteracting Thirring model discussed in Section 2.3. This demonstrates a fundamental difference of our approach to perturbative scaling, where the scaling trajectories go right through the line $\beta^2 = 4\pi$ (see Fig. 1).

3.4.4. H_{diag}

Let us next look at the fifth and sixth term in (57). The total contribution from $[\eta, H_{\text{int}}]$ to terms of this structure is

$$\begin{aligned}
 [\eta, H_{\text{int}}] \longrightarrow & -2i \int dx_1 dx_2 dy_1 dy_2 \frac{\partial u(B; y_1)}{\partial y_1} u(B; y_2) \\
 & \times (s_1^{-\alpha^2} * V_2(-\alpha; x_1 - y_1) V_2(\alpha; x_2 - y_2) * \\
 & - \bar{s}_1^{-\alpha^2} * V_2(\alpha; x_2 - y_2) V_2(-\alpha; x_1 - y_1) * \\
 & + s_1^{-\alpha^2} * V_2(\alpha; x_1 - y_1) V_2(-\alpha; x_2 - y_2) * \\
 & - \bar{s}_1^{-\alpha^2} * V_2(-\alpha; x_2 - y_2) V_2(\alpha; x_1 - y_1) *). \tag{76}
 \end{aligned}$$

For simplicity we will only look at the first term in this expression since all the other terms can be treated likewise. We first exchange the two vertex operators using (A22) as this will lead to a normal-ordered expression below

$$\begin{aligned}
 & -2i \int dx_1 dx_2 dy_1 dy_2 \frac{\partial u(B; y_1)}{\partial y_1} u(B; y_2) s_1^{-\alpha^2} \frac{\bar{s}_2^{\alpha^2}}{s_2^{\alpha^2}} \\
 & \quad \times *V_2(\alpha; x_2 - y_2)V_2(-\alpha; x_1 - y_1)*
 \end{aligned} \tag{77}$$

with s_1, s_2 from (56). We can rewrite this in terms of Fourier transforms ($\alpha > 0$)

$$V_j(-\alpha; x) \stackrel{\text{def}}{=} \sum_p e^{ipx} V_j(-\alpha; p), \quad V_j(\alpha; p) \stackrel{\text{def}}{=} [V_j(-\alpha; p)]^\dagger, \tag{78}$$

substitute $x_2 \rightarrow x_2 + x_1$ and perform the integral over x_1 . This leads to

$$\begin{aligned}
 & -4\pi i \left(\frac{L}{2\pi}\right)^{\alpha^2} \int dx_2 dy_1 dy_2 \frac{\partial u(B; y_1)}{\partial y_1} u(B; y_2) \\
 & \quad \times \sum_k *V_2(\alpha; k)V_2(-\alpha; k) * (ix_2 + a)^{-\alpha^2} \\
 & \quad \times \frac{[i(x_2 - y_2 + y_1) + a]^{\alpha^2}}{[-i(x_2 - y_2 + y_1) + a]^{\alpha^2}} e^{-ik(x_2+y_1-y_2)} \\
 & \quad = \dots \\
 & \quad = -8\pi^2 \left(\frac{L}{2\pi}\right)^{\alpha^2} \int dx dy \sum_{k,p} p u^2(B; p) e^{-ikx+ipy} * V_2(\alpha; k)V_2(-\alpha; k) * \\
 & \quad \quad \quad \times [i(x+y) + a]^{-\alpha^2} \frac{[ix+a]^{\alpha^2}}{[-ix+a]^{\alpha^2}},
 \end{aligned} \tag{79}$$

where we have employed (46). Next the y -integration can be done using

$$\int dy (iy + ix + a)^{-\alpha^2} e^{ipy} = e^{-ipx} |p|^{\alpha^2-1} \frac{2\pi}{\Gamma(\alpha^2)} \theta(p), \tag{80}$$

which is valid in the limit $|ap| \ll 1$: this holds except for an (unimportant) initial transient with wavevectors of order a^{-1} . We find

$$\begin{aligned}
 & -\frac{16\pi^3}{\Gamma(\alpha^2)} \left(\frac{L}{2\pi}\right)^{\alpha^2} \int dx \sum_k \sum_{p>0} p^{\alpha^2} u^2(B; p) e^{-i(k+p)x} \\
 & \quad \quad \quad \times *V_2(\alpha; k)V_2(-\alpha; k) * \frac{[ix+a]^{\alpha^2}}{[-ix+a]^{\alpha^2}}.
 \end{aligned} \tag{81}$$

Next we can approximate

$$\frac{[ix+a]^{\alpha^2}}{[-ix+a]^{\alpha^2}} \rightarrow \cos(\pi\alpha^2) + i \sin(\pi\alpha^2) \operatorname{sgn}(x) \tag{82}$$

using the same reasoning as in (A24). This gives

$$\begin{aligned}
 & -\frac{16\pi^3}{\Gamma(\alpha^2)} \left(\frac{L}{2\pi}\right)^{\alpha^2} \left(2\pi \cos(\pi\alpha^2) \sum_{k>0} k^{\alpha^2} u^2(B; k) * V_2(\alpha; -k)V_2(-\alpha; -k) * \right. \\
 & \quad \quad \quad \left. + i \sin(\pi\alpha^2) \sum_k \sum_{p>0} p^{\alpha^2} u^2(B; p) \right)
 \end{aligned}$$

$$\begin{aligned}
 & \times \int dx e^{-i(k+p)x} \text{sgn}(x) * V_2(\alpha; -k) V_2(-\alpha; -k) * \\
 & = -2a\alpha^{2-4} \frac{\tilde{u}^2(B)}{\Gamma(\alpha^2)} \left(\frac{2\pi a}{L}\right)^{\alpha^2} \\
 & \times \left(\cos(\pi\alpha^2) \sum_{k>0} k^{\alpha^2} v^2(B; k) * V_2(\alpha; -k) V_2(-\alpha; -k) * \right. \\
 & \quad \left. + \frac{1}{\pi} \sin(\pi\alpha^2) \sum_k \sum_{\substack{p>0 \\ p \neq k}} p^{\alpha^2} v^2(B; p) \frac{1}{p-k} * V_2(\alpha; -k) V_2(-\alpha; -k) * \right).
 \end{aligned} \tag{83}$$

In order to do the sum over p in the second term it will be sufficient to use the approximate solution $v(B; p) = e^{-4Bp^2}$ from (49). Deviations from this approximate solution essentially only occur close to the strong-coupling fixed point $\alpha^2 = 1$, where the second term vanishes anyway. This p -summation leads to an integral of the type

$$\begin{aligned}
 h(\alpha^2; x) &= P \int_0^\infty dy e^{-y^2} \frac{y^{\alpha^2}}{y-x} \\
 &= \frac{1}{2} e^{-x^2} |x|^{\alpha^2} \text{Re} \left\{ i^{\alpha^2} \left[\Gamma\left(1 + \frac{\alpha^2}{2}\right) \Gamma\left(-\frac{\alpha^2}{2}, -x^2\right) \right. \right. \\
 & \quad \left. \left. - i \text{sgn}(x) \Gamma\left(\frac{1+\alpha^2}{2}\right) \Gamma\left(\frac{1-\alpha^2}{2}, -x^2\right) \right] \right\},
 \end{aligned} \tag{84}$$

where $\Gamma(s, z)$ denotes the incomplete Γ -function. One easily shows $h(\alpha^2; x = 0) = \Gamma(\alpha^2/2)/2$ and the asymptotic behavior for $|x| \gg 1$

$$h(\alpha^2; x) = -\frac{\Gamma\left(\frac{1+\alpha^2}{2}\right)}{2x} + O(x^{-2}) \tag{85}$$

with a smooth crossover in between.

It will be convenient to use the normalized operators

$$\begin{aligned}
 S_j(\alpha; k) &\stackrel{\text{def}}{=} \left[\frac{2\pi}{L} \Gamma(\alpha^2) \left(\frac{L|k|}{2\pi}\right)^{1-\alpha^2} \right]^{1/2} V_j(-\alpha; k) \\
 \Rightarrow S_j^\dagger(\alpha; k) &= \left[\frac{2\pi}{L} \Gamma(\alpha^2) \left(\frac{L|k|}{2\pi}\right)^{1-\alpha^2} \right]^{1/2} V_j(\alpha; k)
 \end{aligned} \tag{86}$$

with the properties (see (A7))

$$S_1^\dagger(\alpha; -k)|\Omega\rangle = S_1(\alpha; k)|\Omega\rangle = S_2^\dagger(\alpha; k)|\Omega\rangle = S_2(\alpha; -k)|\Omega\rangle = 0 \quad \forall k > 0 \tag{87}$$

and the normalization

$$\begin{aligned}
 \langle S_1(\alpha; k) S_1^\dagger(\alpha; k') \rangle &= \langle S_2^\dagger(\alpha; k) S_2(\alpha; k') \rangle = \delta_{kk'} \theta(k) L/2\pi, \\
 \langle S_1^\dagger(\alpha; k) S_1(\alpha; k') \rangle &= \langle S_2(\alpha; k) S_2^\dagger(\alpha; k') \rangle = \delta_{kk'} \theta(-k) L/2\pi
 \end{aligned} \tag{88}$$

for $|ak|, |ak'| \ll 1$ as follows easily from (A16) and (A17). We express (83) in terms of these operators and find

$$\begin{aligned}
 & -\frac{2\tilde{u}^2(B)}{a^3\Gamma^2(\alpha^2)} \left(\cos(\pi\alpha^2) \sum_{k>0} (ak)^{2\alpha^2-1} v^2(B; k) S_2^\dagger(\alpha; -k) S_2(\alpha; -k) \right. \\
 & + \frac{1}{\pi} \sin(\pi\alpha^2) \sum_{k>0} (ak)^{\alpha^2-1} (8B/a^2)^{-\alpha^2/2} h(\alpha^2; \sqrt{8B}k) S_2^\dagger(\alpha; -k) S_2(\alpha; -k) \\
 & \left. + \frac{1}{\pi} \sin(\pi\alpha^2) \sum_{k>0} (ak)^{\alpha^2-1} (8B/a^2)^{-\alpha^2/2} h(\alpha^2; \sqrt{8B}k) * S_2^\dagger(\alpha; k) S_2(\alpha; k) * \right). \tag{89}
 \end{aligned}$$

In the first two terms we do not need the subtraction operation $*$ $*$ anymore since the vacuum is already annihilated by them. The third term does not yet annihilate the vacuum. This can be easily achieved by using (A26). However, already the second term will turn out to have hardly any effect, and the third term is again smaller than the second term. In order to simplify our expressions we therefore omit the third term in the sequel, although there would be no problem at all in carrying it along as well. Let us now also collect the other terms from (76) leading to

$$\begin{aligned}
 [\eta, H_{\text{int}}] & \longrightarrow -\frac{4\tilde{u}^2(B)}{a^3\Gamma^2(\alpha^2)} \\
 & \times \sum_{k>0} \left(\cos(\pi\alpha^2) (ak)^{2\alpha^2-1} v^2(B; k) \right. \\
 & \quad \left. + \frac{1}{\pi} \sin(\pi\alpha^2) (ak)^{\alpha^2-1} (8B/a^2)^{-\alpha^2/2} h(\alpha^2; \sqrt{8B}k) \right) \\
 & \times (S_1(\alpha; -k) S_1^\dagger(\alpha; -k) + S_1^\dagger(\alpha; k) S_1(\alpha; k) \\
 & \quad + S_2^\dagger(\alpha; -k) S_2(\alpha; -k) + S_2(\alpha; k) S_2^\dagger(\alpha; k)). \tag{90}
 \end{aligned}$$

Since α generically flows as a function of B , this implies that vertex operators with different scaling dimensions contribute to each wavevector k . However, most of the contribution to a given k -vector occurs in a narrow range of the flow: we will see in Section 4.3 that for a given k the main contribution occurs when $B \approx B_k$ with

$$\begin{aligned}
 B_k & \stackrel{\text{def}}{=} \frac{1}{4k^2} && \text{(weak-coupling phase),} \\
 B_k & \stackrel{\text{def}}{=} \frac{1}{4k\sqrt{k^2 + M^2}} && \text{(strong-coupling phase with mass gap } M\text{).} \tag{91}
 \end{aligned}$$

In order to simplify our notation we therefore use a single scaling dimension α corresponding to each k with $\alpha = \alpha(B_k)$.³ The newly generated term in the Hamiltonian can then be written as

³ This approximation becomes exact in the low-energy limit, e.g., in the strong-coupling phase for $|k| \ll M$.

$$H_{\text{diag}}(B) = \sum_{k>0} \omega(B; k) (P_1(-k)P_1^\dagger(-k) + P_1^\dagger(k)P_1(k) + P_2^\dagger(-k)P_2(-k) + P_2(k)P_2^\dagger(k)) \tag{92}$$

with

$$P_j(k) \stackrel{\text{def}}{=} S_j(\alpha(B_k); k), \quad P_j^\dagger(k) = S_j^\dagger(\alpha(B_k); k) \tag{93}$$

and according to (90)

$$\frac{\partial \omega(B; k)}{\partial B} = -\frac{4\tilde{u}^2(B)}{a^3 \Gamma^2(\alpha^2)} \left(\cos(\pi \alpha^2) (ak)^{2\alpha^2-1} v^2(B; k) + \frac{1}{\pi} \sin(\pi \alpha^2) (ak)^{\alpha^2-1} (8B/a^2)^{-\alpha^2/2} h(\alpha^2; \sqrt{8B}k) \right) \tag{94}$$

with $\omega(B = 0; k) = 0$. Using Eqs. (42) one can easily check $[H_0, H_{\text{diag}}(B)] = 0$, therefore $H_{\text{diag}}(B)$ can be interpreted as diagonal.

3.4.5. H_{res}

So far we have not discussed the commutators with the structure $[V_1 V_2^\dagger, V_1 V_2^\dagger]$ and $[V_1^\dagger V_2, V_1^\dagger V_2]$ that are also generated by $[\eta, H_{\text{int}}]$. From (51) one concludes that these commutators contain only the R -term. The operator product expansion in the R -term then generates interactions with the structure $V_1(2\alpha)V_2(-2\alpha)$, etc., that is only terms with larger scaling dimensions. These interactions are neglected in the present approximation, just like the higher-order terms in (59). We formally sum up these neglected terms with larger scaling dimensions in H_{res} .

3.5. Commutator $[\eta, H_{\text{diag}}]$

We also have to study the effect of the infinitesimal unitary transformations on the newly generated terms (92). An overlap exists essentially only for wavevectors of order $B^{-1/2}$. For notational simplicity we can therefore use the running scaling dimension $\alpha = \alpha(B)$ in (92) and arrive at the following commutator

$$[\eta, H_{\text{diag}}] = -2i \int dx dy \frac{\partial u(B; y)}{\partial y} \times \sum_{k>0} \omega(B; k) \left([V_1(\alpha; x)V_2(-\alpha; x-y), S_1(\alpha; -k)S_1^\dagger(\alpha; -k) + S_1^\dagger(\alpha; k)S_1(\alpha; k) + S_2^\dagger(\alpha; -k)S_2(\alpha; -k) + S_2(\alpha; k)S_2^\dagger(\alpha; k)] + \text{h.c.} \right). \tag{95}$$

A typical contribution comes, e.g., from

$$[V_1(\alpha; x), S_1^\dagger(\alpha; k)S_1(\alpha; k)] = V_1(\alpha; x)S_1^\dagger(\alpha; k)S_1(\alpha; k) - S_1^\dagger(\alpha; k) * S_1(\alpha; k)V_1(\alpha; x) * - S_1^\dagger(\alpha; k)\langle S_1(\alpha; k)V_1(\alpha; x) \rangle. \tag{96}$$

The first and the second term on the rhs lead to normal-ordered interactions with larger scaling dimensions and are therefore neglected (or formally contained in H_{res}). The third term on the rhs gives rise to interactions of the type H_{int} leading to

$$\begin{aligned}
 [\eta, H_{\text{diag}}] &\longrightarrow -2i \int dx dy \frac{\partial u(B; y)}{\partial y} \\
 &\quad \times \sum_{k>0} \omega(B; k) \left(V_1(\alpha; x) S_2(\alpha; -k) \langle V_2(-\alpha; x-y) S_2^\dagger(\alpha; -k) \right. \\
 &\quad \quad - V_1(\alpha; x) S_2(\alpha; k) \langle S_2^\dagger(\alpha; k) V_2(-\alpha; x-y) \rangle \\
 &\quad \quad + \langle V_1(\alpha; x) S_1(\alpha; -k) \rangle S_1^\dagger(\alpha; -k) V_2(-\alpha; x-y) \\
 &\quad \quad \left. - \langle S_1(\alpha; k) V_1(\alpha; x) \rangle S_1^\dagger(\alpha; k) V_2(-\alpha; x-y) + \text{h.c.} \right) \\
 &= -2i \int dx dy \frac{\partial u(B; y)}{\partial y} \sum_{k>0} \omega(B; k) \left[\Gamma(\alpha^2) \frac{2\pi}{L} \left(\frac{L|k|}{2\pi} \right)^{1-\alpha^2} \right]^{-1/2} \\
 &\quad \times \left(V_1(\alpha; x) S_2(\alpha; -k) e^{-ik(x-y)} - V_1(\alpha; x) S_2(\alpha; k) e^{ik(x-y)} \right. \\
 &\quad \quad + S_1^\dagger(\alpha; -k) V_2(-\alpha; x-y) e^{ikx} \\
 &\quad \quad \left. - S_1^\dagger(\alpha; k) V_2(-\alpha; x-y) e^{-ikx} + \text{h.c.} \right) \\
 &= -4\pi \int dx \sum_{k>0} \omega(B; k) k u(B; k) \left[\Gamma(\alpha^2) \frac{2\pi}{L} \left(\frac{L|k|}{2\pi} \right)^{1-\alpha^2} \right]^{-1/2} \\
 &\quad \times \left(V_1(\alpha; x) S_2(\alpha; -k) e^{-ikx} + V_1(\alpha; x) S_2(\alpha; k) e^{ikx} \right. \\
 &\quad \quad \left. + S_1^\dagger(\alpha; -k) V_2(-\alpha; x) e^{ikx} + S_1^\dagger(\alpha; k) V_2(-\alpha; x) e^{-ikx} + \text{h.c.} \right) \\
 &= -8\pi L \sum_k \omega(B; |k|) |k| u(B; k) \frac{1}{\Gamma(\alpha^2)} \left(\frac{L|k|}{2\pi} \right)^{\alpha^2-1} \\
 &\quad \times \left(S_1^\dagger(\alpha; k) S_2(\alpha; k) + S_2^\dagger(\alpha; k) S_1(\alpha; k) \right). \tag{97}
 \end{aligned}$$

This term has to be compared with (39)

$$\begin{aligned}
 H_{\text{int}} &= \int dx dy u(B; y) \left(V_1(\alpha; x) V_2(-\alpha; x-y) + \text{h.c.} \right) \\
 &= 2\pi L \sum_k u(B; k) \frac{1}{\Gamma(\alpha^2)} \left(\frac{L|k|}{2\pi} \right)^{\alpha^2-1} \left(S_1^\dagger(\alpha; k) S_2(\alpha; k) + S_2^\dagger(\alpha; k) S_1(\alpha; k) \right). \tag{98}
 \end{aligned}$$

Eq. (97) therefore gives an additional contribution to the previous flow equation (49) and one finds

$$\frac{\partial v(B; k)}{\partial B} = -4k^2 v(B; k) - 4|k| \omega(B; |k|) v(B; k). \tag{99}$$

3.6. Flow of β^2

3.6.1. Unitary transformation e^U

We have seen that the term (75)

$$\sum_k w_k(B) |k| \sigma_1(k) \sigma_2(-k) dB \tag{100}$$

with

$$w_k(B) = \frac{32}{a^2} \left(\frac{32B}{a^2} \right)^{1-\alpha^2(B)} \frac{\alpha^2(B)}{2\Gamma(\alpha^2(B) - 1)} \tilde{u}^2(B) f(\alpha^2(B); k\sqrt{B}) \tag{101}$$

is generated during the flow. This term is not contained in the original sine-Gordon Hamiltonian. We will now show how this term can be eliminated by an additional unitary transformation e^U with

$$U = \sum_{p>0} \psi_p (\sigma_1(p) \sigma_2(-p) - \sigma_1(-p) \sigma_2(p)) \tag{102}$$

with suitable parameters ψ_p [29].

Let us first write down some general properties of this unitary transformation for general ψ_p . The bosonic fields are transformed according to

$$\begin{aligned} e^{-U} \sigma_1(p) e^U &= \sigma_1(p) \cosh \psi_p + \sigma_2(p) \sinh \psi_p, \\ e^{-U} \sigma_2(p) e^U &= \sigma_2(p) \cosh \psi_p + \sigma_1(p) \sinh \psi_p \end{aligned} \tag{103}$$

and vertex operators as

$$\begin{aligned} e^{-U} V_1(\alpha; x) e^U &= e^C : \exp \left[\alpha \sum_{p \neq 0} \cosh \psi_p \frac{\sqrt{|p|}}{p} e^{-\frac{\alpha}{2}|p| - ipx} \sigma_1(p) \right] : \\ &\quad \times : \exp \left[\alpha \sum_{p \neq 0} \sinh \psi_p \frac{\sqrt{|p|}}{p} e^{-\frac{\alpha}{2}|p| - ipx} \sigma_2(p) \right] :, \\ e^{-U} V_2(\alpha; x) e^U &= e^C : \exp \left[-\alpha \sum_{p \neq 0} \cosh \psi_p \frac{\sqrt{|p|}}{p} e^{-\frac{\alpha}{2}|p| - ipx} \sigma_2(p) \right] : \\ &\quad \times : \exp \left[-\alpha \sum_{p \neq 0} \sinh \psi_p \frac{\sqrt{|p|}}{p} e^{-\frac{\alpha}{2}|p| - ipx} \sigma_1(p) \right] :, \end{aligned} \tag{104}$$

where

$$C = -\alpha^2 \sum_{p>0} \sinh \psi_p \sinh \psi_{-p} \frac{e^{-a|p|}}{p}. \tag{105}$$

3.6.2. $e^{-U} H e^U$

We take the point of view that (100) has been generated infinitesimally by integrating the flow equations from B to $B + dB$. We therefore apply the above unitary transformation (102) to H

$$H(B + dB) \longrightarrow e^{-U} H(B + dB)e^U. \tag{106}$$

Let us first investigate the effect on H_0 : for the choice

$$\psi_p = -\frac{w_p(B)}{2}dB, \tag{107}$$

the transformation $e^{-U} H_0 e^U$ reproduces H_0 and generates an additional term that annihilates (100). This can be shown easily by using the transformation rules (103). Notice that terms of order ψ_p^2 and higher can be neglected since ψ_p is of order dB .

Next we have to find the effect of this transformation on $H_{\text{int}}(B)$. Using (104) one finds

$$\begin{aligned} & e^{-U} V_1(\alpha; x) V_2(-\alpha; y) e^U \\ &= V_1(\alpha; x) : \exp \left[\alpha \sum_{p \neq 0} \psi_p \frac{\sqrt{|p|}}{p} e^{-\frac{\alpha}{2}|p| - ipy} \sigma_1(p) \right] : \\ & \times V_2(-\alpha; y) : \exp \left[\alpha \sum_{p \neq 0} \psi_p \frac{\sqrt{|p|}}{p} e^{-\frac{\alpha}{2}|p| - ipx} \sigma_2(p) \right] :, \end{aligned} \tag{108}$$

where we have again used that ψ_p is of order dB . Using an OPE, we can combine the first two terms into a vertex operator with a modified scaling dimension, and likewise for the second two terms. The calculation proceeds along similar lines as in (A18):

$$\begin{aligned} & V_1(\alpha; x) : \exp \left[\alpha \sum_{p \neq 0} \psi_p \frac{\sqrt{|p|}}{p} e^{-\frac{\alpha}{2}|p| - ipy} \sigma_1(p) \right] : \\ &= \exp \left[\alpha \sum_{p > 0} \frac{\sqrt{|p|}}{p} e^{-\frac{\alpha}{2}|p| - ipx} \sigma_1(p) \right] \exp \left[\alpha \sum_{p < 0} \frac{\sqrt{|p|}}{p} e^{-\frac{\alpha}{2}|p| - ipx} \sigma_1(p) \right] \\ & \times \exp \left[\alpha \sum_{p > 0} \psi_p \frac{\sqrt{|p|}}{p} e^{-\frac{\alpha}{2}|p| - ipy} \sigma_1(p) \right] \\ & \times \exp \left[\alpha \sum_{p < 0} \psi_p \frac{\sqrt{|p|}}{p} e^{-\frac{\alpha}{2}|p| - ipy} \sigma_1(p) \right] \\ &= e^C \times \exp \left[\alpha \sum_{p > 0} \frac{\sqrt{|p|}}{p} e^{-\frac{\alpha}{2}|p| - ipx} (1 + \psi_p e^{-ip(y-x)}) \sigma_1(p) \right] \\ & \times \exp \left[\alpha \sum_{p < 0} \frac{\sqrt{|p|}}{p} e^{-\frac{\alpha}{2}|p| - ipx} (1 + \psi_p e^{-ip(y-x)}) \sigma_1(p) \right], \end{aligned} \tag{109}$$

where

$$C = -\alpha^2 \sum_{p > 0} \psi_p \frac{\exp(-ap - ip(x - y))}{p}. \tag{110}$$

From (74) we know that ψ_p falls off rapidly on an energy scale of order $B^{-1/2}$. The leading behavior of the sum is therefore (except for an uninteresting initial transient)

$$C = -\alpha^2 \psi_{p=0} \sum_{p>0} \frac{\exp(-\tilde{a}p - ip(x-y))}{p} \tag{111}$$

leading to (compare Eq. (A13))

$$e^C = \left(\frac{2\pi(\tilde{a} + i(x-y))}{L} \right)^{\alpha^2 \psi_{p=0}}. \tag{112}$$

Here $\tilde{a} = s\sqrt{B}$ takes into account the UV-cutoff generated by the decay of the functions $f(\alpha^2; x)$ from Fig. 2. The actual value of the proportionality constant s will only affect our results in next to leading order as will be shown later. Still we give its value here for latter comparison with the three loop scaling results: for $\alpha^2 = 2$ one finds in a somehow lengthy calculation

$$\ln s = \ln 2 + \frac{\pi}{4} - \frac{\gamma}{2}, \tag{113}$$

where $\gamma \approx 0.577$ is Euler’s constant. s depends only weakly on α^2 , therefore we will use this value throughout. Next

$$\begin{aligned} & \exp \left[\alpha \sum_{p>0} \frac{\sqrt{|p|}}{p} e^{-\frac{a}{2}|p|-ipx} (1 + \psi_p e^{-ip(y-x)}) \sigma_1(p) \right] \\ &= \exp \left[\alpha(1 + \psi_{p=0}) \sum_{p>0} \frac{\sqrt{|p|}}{p} e^{-\frac{a}{2}|p|-ipx} \sigma_1(p) \right] \\ & \quad \times \exp \left[i(x-y)\alpha\psi_{p=0} \sum_{p>0} \sqrt{|p|} e^{-\frac{a}{2}|p|-ipx} \sigma_1(p) + O((x-y)^2) \right] \\ &= V_1(\alpha(1 + \psi_{p=0}); x) \\ & \quad \times \left(1 + i(x-y)\alpha\psi_{p=0} \sum_{p>0} \sqrt{|p|} e^{-\frac{a}{2}|p|-ipx} \sigma_1(p) + O((x-y)^2) \right) \\ &= V_1(\alpha(1 + \psi_{p=0}); x) + \text{more irrelevant terms} \end{aligned} \tag{114}$$

up to less singular (more irrelevant) terms. We formally include these more irrelevant terms (they have the structure of products of vertex operators multiplied by derivatives of the bosonic field) into H_{res} and neglect them from now on. It should also be noted that we have approximated the flow of the scaling dimension in the vertex operator by restricting ourselves to the flow in the IR-limit $\alpha \rightarrow \alpha(1 + \psi_{p=0})$. At first sight this seems to be a problematic approximation since the functions $f(\alpha^2; x)$ in (74) are nontrivial. However, the effect of the unitary transformations is *only* cumulative on the low-energy scale where $f(\alpha^2; x) \xrightarrow{x \rightarrow 0} 1$. Hence it is possible to restrict ourselves to the IR-limit.

Putting everything together we find

$$\begin{aligned} H_{\text{int}}(B + dB) &\longrightarrow e^{-U} H_{\text{int}}(B + dB) e^U \\ &= \left(\frac{2\pi s\sqrt{B}}{L} \right)^{-\alpha^2(B)w_{p=0}(B)dB} \end{aligned}$$

$$\begin{aligned} & \times \int dx dy u(B; y) \\ & \times [V_1(\alpha(1 - \frac{w_{p=0}(B)}{2} dB); x) \\ & \times V_2(-\alpha(1 - \frac{w_{p=0}(B)}{2} dB); x - y) + \text{h.c.}]. \end{aligned} \tag{115}$$

Similar to the OPE above we have set $x - y = 0$ in (112), that is we have neglected less singular terms.

Finally, we have to investigate the effect of the additional unitary transformation (106) on H_{diag} from (92). This is similar to the action on the interaction term, except that here we find terms of the structure

$$\begin{aligned} & e^{-U} V_1(\alpha; x) V_1(-\alpha; y) e^U \\ & = V_1(\alpha; x) V_1(-\alpha; y) : \exp \left[\alpha \sum_{p \neq 0} \psi_p \frac{\sqrt{|p|}}{p} e^{-\frac{g}{2}|p| - ipx} \sigma_2(p) \right] : \\ & \times : \exp \left[-\alpha \sum_{p \neq 0} \psi_p \frac{\sqrt{|p|}}{p} e^{-\frac{g}{2}|p| - ipy} \sigma_2(p) \right] : \end{aligned} \tag{116}$$

and likewise for $j = 2$. The third and fourth term can be combined using an OPE (A19) and one easily notices that the only surviving term is a constant 1 since all other terms are of order $\psi_p^2 = O(dB^2)$. Hence

$$H_{\text{diag}}(B + dB) \longrightarrow e^{-U} H_{\text{diag}}(B + dB) e^U = H_{\text{diag}}(B + dB). \tag{117}$$

Summing up, we have looked at another infinitesimal unitary transformation (106) that acts on the Hamiltonian during the flow equation procedure in addition to the generator (43). An alternative viewpoint is to say that the full generator of the flow now takes the structure

$$\begin{aligned} \eta_{\text{new}}(B) & = -2i \int dx dy \frac{\partial u(B; y)}{\partial y} (V_1(\alpha; x) V_2(-\alpha; x - y) + \text{h.c.}) \\ & + \frac{1}{2} \sum_p w_p(B) (\sigma_1(p) \sigma_2(-p) - \sigma_1(-p) \sigma_2(p)). \end{aligned} \tag{118}$$

3.6.3. Flow equation for β^2

From (115) we can read of that the additional infinitesimal unitary transformation generates a flow in the scaling dimension of the vertex operators

$$\begin{aligned} & \alpha(B) \longrightarrow \alpha(B) \left(1 - \frac{w_{p=0}(B)}{2} dB \right) \\ \Rightarrow \frac{d\alpha^2}{dB} & = -w_{p=0}(B) \alpha^2(B) = -\frac{32}{a^2} \left(\frac{32B}{a^2} \right)^{1-\alpha^2(B)} \frac{\alpha^4(B)}{2\Gamma(\alpha^2(B) - 1)} \tilde{u}^2(B). \end{aligned} \tag{119}$$

We can already see that $\alpha^2 = 1$ is a fixed point of the flow equation approach due to the diverging Γ -function in the denominator of (119). *This will be one of the key results of our new approach.*

According to (115) this flow of the scaling dimension now induces a flow of the coupling constant $u(B; y)$

$$\begin{aligned} u(B; y) &\longrightarrow u(B; y) \left(\frac{2\pi s \sqrt{B}}{L} \right)^{-\alpha^2(B)w_{p=0}(B)dB} \\ &= u(B; y) \left(1 - \alpha^2(B)w_{p=0}(B)dB \ln \left(\frac{2\pi s \sqrt{B}}{L} \right) \right) \\ \Rightarrow \frac{du(B; y)}{dB} &= u(B; y) \frac{d\alpha^2}{dB} \ln \left(\frac{2\pi s \sqrt{B}}{L} \right). \end{aligned} \tag{120}$$

The solution is straightforward

$$\begin{aligned} u(B; y) &= u(B=0; y) \exp \left(\int_0^B dB' \frac{d\alpha^2}{dB'} \ln \left(\frac{2\pi s \sqrt{B'}}{L} \right) \right) \\ &= u(B=0; y) \exp \left(\int_0^B dB' \frac{d\alpha^2}{dB'} \ln \left(\frac{2\pi a}{L} \sqrt{\frac{32B'}{a^2}} \frac{s}{\sqrt{32}} \right) \right) \\ &= u(B=0; y) \left(\frac{2\pi a}{L} \right)^{\alpha^2(B)-\alpha^2(0)} \left(\frac{s}{\sqrt{32}} \right)^{\alpha^2(B)-\alpha^2(0)} \\ &\quad \times \exp \left(\frac{1}{2} \int_0^B dB' \frac{d\alpha^2}{dB'} \ln \left(\frac{32B'}{a^2} \right) \right). \end{aligned} \tag{121}$$

Using the parametrization (48)

$$u(B; p) = \frac{\tilde{u}(B)}{4\pi^2 a^2} \left(\frac{2\pi a}{L} \right)^{\alpha^2(B)} v(B; p) \tag{122}$$

we see that this can be most conveniently expressed as a flow equation for the *running coupling constant* $\tilde{u}(B)$ in (122)

$$\tilde{u}(B) = u_0 \left(\frac{s}{\sqrt{32}} \right)^{\alpha^2(B)-\alpha^2(0)} \exp \left(\frac{1}{2} \int_0^B dB' \frac{d\alpha^2}{dB'} \ln \left(\frac{32B'}{a^2} \right) \right). \tag{123}$$

Introducing the dimensionless logarithmic flow parameter ℓ

$$\ell \stackrel{\text{def}}{=} \frac{1}{2} \ln \left(\frac{32B}{a^2} \right), \tag{124}$$

one can show by partial integration

$$\frac{1}{2} \int_0^B dB' \frac{d\alpha^2}{dB'} \ln \left(\frac{32B'}{a^2} \right) = - \int_0^\ell d\ell' \alpha^2(\ell') + \alpha^2(\ell) \ell. \tag{125}$$

Using this we can sum up the results of this section in the following two equations:

$$\tilde{u}(\ell) = u_0 \left(\frac{s}{\sqrt{32}} \right)^{\alpha^2(\ell) - \alpha^2(0)} \exp \left(- \int_0^\ell d\ell' \alpha^2(\ell') + \alpha^2(\ell) \ell \right), \tag{126}$$

$$\frac{d\alpha^2}{d\ell} = -u_0^2 \left(\frac{s^2}{32} \right)^{\alpha^2(\ell) - \alpha^2(0)} \frac{\alpha^4(\ell)}{\Gamma(\alpha^2(\ell) - 1)} \exp \left(4\ell - 2 \int_0^\ell d\ell' \alpha^2(\ell') \right). \tag{127}$$

These two equations constitute the key results of this work. Eq. (127) describes the flow of the scaling dimension under the flow equation procedure, and from Eq. (126) it follows how this induces the flow of the running coupling constant $\tilde{u}(\ell)$. Therefore these equations will serve as a generalization of the scaling equations derived in perturbative renormalization theory in Section 2.2. The value of the constant s in these equations will turn out to affect our results only in next to leading order.

4. Solution of the flow equations

4.1. Summary of the flow equations

In this section we will sum up the results for the flow of the sine-Gordon Hamiltonian under the effect of the infinitesimal unitary transformation (118) as derived above. For general B the sequence $H(B)$ of unitarily equivalent Hamiltonians takes the form

$$H(B) = H_0 + H_{\text{int}}(B) + H_{\text{diag}}(B) + H_{\text{res}}(B). \tag{128}$$

Here

$$H_0 = \int dx \left(\frac{1}{2} \Pi^2(x) + \frac{1}{2} \left(\frac{\partial \phi}{\partial x} \right)^2 \right), \tag{129}$$

$$H_{\text{int}}(B) = \int dx dy u(B; y) (V_1(\alpha(B); x) V_2(-\alpha(B); x - y) + \text{h.c.}), \tag{130}$$

$$H_{\text{diag}}(B) = \sum_{k>0} \omega(B; k) (P_1(-k) P_1^\dagger(-k) + P_1^\dagger(k) P_1(k) + P_2^\dagger(-k) P_2(-k) + P_2(k) P_2^\dagger(k)), \tag{131}$$

with $P_j(k)$ given by (93)

$$P_j(k) = \left[\frac{\Gamma(\alpha^2(B_k))}{2\pi L} \left(\frac{L|k|}{2\pi} \right)^{1 - \alpha^2(B_k)} \right]^{1/2} \int dx e^{-ikx} V_j(-\alpha(B_k); x) \tag{132}$$

and B_k from (91). The operators $P_j(k)$, $P_j^\dagger(k)$ will turn out to be the soliton creation and annihilation operators. They are normalized according to (88). Notice $H_{\text{diag}}(B)|\Omega\rangle = 0$.

H_{res} contains the neglected terms and will from now on be omitted in our analysis. At any given B -scale these neglected terms have a larger scaling dimension than the interaction term $H_{\text{int}}(B)$: they are more irrelevant by at least two spatial derivatives. Notice that H_{res} vanishes for $\beta^2 = 4\pi$ since then no approximations are made.

Summing up the differential flow equations for the parameters in $H(B)$ we have

$$\begin{aligned} \frac{\partial v(B; k)}{\partial B} &= -4k^2 v(B; k) - 4k \omega(B; k) v(B; k), \\ \frac{\partial(a \omega(B; k))}{\partial(B/a^2)} &= -\frac{4\tilde{u}^2(B)}{\Gamma^2(\alpha^2)} \left(\cos(\pi \alpha^2) (ak)^{2\alpha^2-1} v^2(B; k) \right. \\ &\quad \left. + \frac{1}{\pi} \sin(\pi \alpha^2) (ak)^{\alpha^2-1} (8B/a^2)^{-\alpha^2/2} h(\alpha^2; \sqrt{8Bk}) \right) \end{aligned} \tag{133}$$

$$\tag{134}$$

for $k > 0$, and $v(B; -k) = v(B; k)$ symmetric in k . For notational convenience we have written $\alpha(B)$ without its argument B in these equations. $h(\alpha^2; x)$ has been defined in (84) and

$$u(B; y) = \frac{\tilde{u}(B)}{4\pi^2 a^2} \left(\frac{2\pi a}{L} \right)^{\alpha^2(B)} \sum_p v(B; p) e^{-ipy}. \tag{135}$$

The initial conditions are $H_{\text{res}}(B = 0) = 0$, $\omega(B = 0; k) = 0$ and $v(B = 0; k) = 1$, whereupon (128) takes the form (18) of our original sine-Gordon Hamiltonian. For $\alpha_0^2 < 1$ one should in fact be more cautious and start the integration only at $B = a^2$: the above equations hold only for $B \gtrsim a^2$ since we have used $|ak| \gg 1$ in our calculation. One can easily verify that there is no flow of the parameters for $B \ll a^2$, and the simplest way to take this into account is to pose the initial conditions at $B = a^2$.

As we will see later the flow of the parameters is such that $v(B = \infty; k) = 0$ for $\beta_0^2 > 2\pi$. In this parameter region the Hamiltonian $H(B)$ from (128) therefore becomes diagonal with $H_{\text{int}}(B = \infty) = 0$ in the limit $B \rightarrow \infty$ as expected under the flow equation procedure

$$H(B = \infty) = H_0 + H_{\text{diag}}(B = \infty), \tag{136}$$

notice $[H_0, H_{\text{diag}}(B)] = 0$.

Eqs. (133) and (134) have to be supplemented with the differential equation governing the flow of the scaling dimension (127) and the thereby induced flow of the running coupling constant (126). It is possible to rewrite (127) in a more conventional form for comparison with the perturbative scaling approach. Introducing a new function

$$u(\ell) \stackrel{\text{def}}{=} u_0 \left(\frac{s}{\sqrt{32}} \right)^{\alpha^2(\ell) - \alpha^2(0)} \exp \left(2\ell - \int_0^\ell d\ell' \alpha^2(\ell') \right) \tag{137}$$

we can rewrite (127) as a set of two coupled differential equations

$$\frac{d\alpha^2}{d\ell} = -\frac{\alpha^4(\ell)}{\Gamma(\alpha^2(\ell) - 1)} u^2(\ell), \tag{138}$$

$$\frac{du}{d\ell} = (2 - \alpha^2(\ell)) u(\ell) + \left(\frac{\pi}{4} - \frac{\gamma}{2} - \frac{1}{2} \ln 8 \right) \frac{d\alpha^2}{d\ell} u(\ell) \tag{139}$$

with the initial conditions $u(\ell = 0) = u_0$ and $\alpha(\ell = 0) = \beta_0/\sqrt{4\pi}$. For convenience we have used the dimensionless flow parameter $\ell = \frac{1}{2} \ln(32B/a^2)$ from (124) in these

equations. Notice that the second term in (139) is of order u^3 and does therefore not contribute to the leading behavior for small u_0 . Since our present flow equation expansion has not taken all the terms in order u^3 into account anyway, we can omit this term and arrive at

$$\frac{d\alpha^2}{d\ell} = -\frac{\alpha^4(\ell)}{\Gamma(\alpha^2(\ell) - 1)} u^2(\ell), \quad \frac{du}{d\ell} = (2 - \alpha^2(\ell)) u(\ell). \quad (140)$$

The running coupling constant $\tilde{u}(\ell)$ from (126) can also be expressed as

$$\tilde{u}(\ell) = u(\ell) \exp((\alpha^2(\ell) - 2)\ell). \quad (141)$$

In terms of the sine-Gordon parameter β these equations take the equivalent form

$$\frac{d\beta^{-2}(\ell)}{d\ell} = \frac{1}{4\pi\Gamma(-1 + \beta^2(\ell)/4\pi)} u^2(\ell), \quad \frac{du}{d\ell} = \left(2 - \frac{\beta^2(\ell)}{4\pi}\right) u(\ell) \quad (142)$$

and

$$\tilde{u}(\ell) = u(\ell) \exp\left(\left(\frac{\beta^2(\ell)}{4\pi} - 2\right)\ell\right). \quad (143)$$

Finally it is of some interest to express $H_{\text{int}}(B)$ directly in terms of the bosonic field $\phi(x)$ and its dual $\Theta(x)$ (see Eq. (11)). After a short calculation one finds

$$\begin{aligned} H_{\text{int}}(B) = \frac{\tilde{u}(B)}{\pi a^2} \int dx dy v(B; y) \\ \times \cos\left(\beta(B) \int d\epsilon c(\epsilon) \frac{1}{2}(\phi(x + \epsilon) + \phi(x - y + \epsilon)) \right. \\ \left. + \Theta(x + \epsilon) - \Theta(x - y + \epsilon)\right). \quad (144) \end{aligned}$$

Since $v(B; y)$ becomes more and more nonlocal during the flow, one sees that the interaction term of the sine-Gordon model evolves from the original $\cos(\beta\phi(x))$ -structure to a nonlocal interaction term with the structure

$$\cos((\beta/2)(\phi(x) + \phi(x - y) + \Theta(x) - \Theta(x - y))). \quad (145)$$

It is also possible to express $H_{\text{diag}}(B)$ in terms of $\phi(x)$ and $\Theta(x)$, however, this expression does not lead to new insights.

4.2. Strong-coupling phase

4.2.1. Fixed points and phase structure

We will now work on the explicit solution of the flow equations (133), (134) and (142). First we focus on the solution of (142), since knowledge of the flow of $\beta(B)$ and $\tilde{u}(B)$ is necessary for solving the system of Eqs. (133) and (134) later on.⁴ From (142) one

⁴ Implicitly an assumption about the behavior of $v(B; k)$ has been made when deriving (142) in Section 3.4. One can check that this assumption is self-consistently justified by analyzing the whole system of equations.

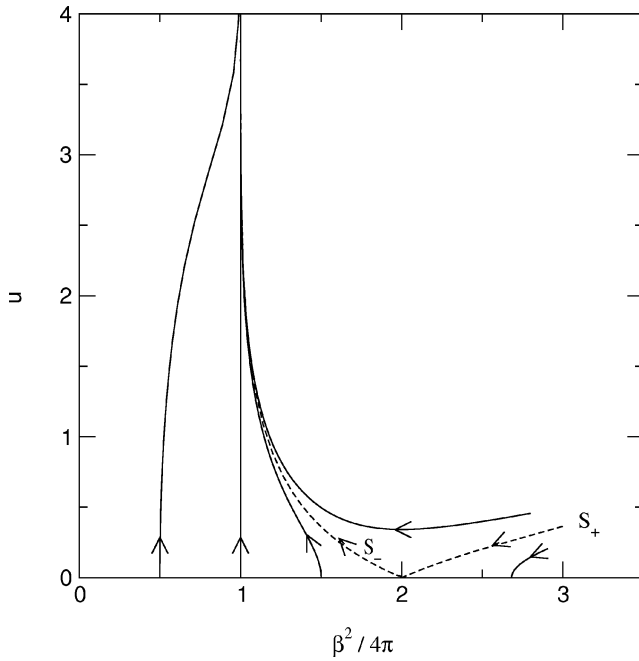


Fig. 3. Scaling flow and the phase diagram of the sine-Gordon model within the flow equation approach. The strong-coupling phase is to the left and/or above the KT-transition line S_+ (dashed line for $\beta^2 \geq 8\pi$), the weak-coupling phase below S_+ . Notice the main difference as compared to the perturbative RG flow (Fig. 1): In the strong-coupling phase $\beta^2 = 4\pi$ is a fixed point of the flow equation approach. The divergence of $u(\ell)$ in the strong-coupling phase is unproblematic within our approach since $\tilde{u}(\ell)$ in Eq. (148) remains *finite* (see text and Section 4.4 where the actual expansion parameter of our approach is analyzed).

concludes that there are two possible kinds of asymptotic behavior: either $\beta^2(\infty) = 4\pi$ or $\beta^2(\infty) \geq 8\pi$. $\beta^2(\infty) = 4\pi$ will turn out to be the *attractive strong-coupling fixed point* and values $\beta^2(\infty) \geq 8\pi$ correspond to the gapless *weak-coupling phase*. These flows and the phase diagram of the sine-Gordon model within the flow equation approach are depicted in Fig. 3. The flow in the strong-coupling phase is consistent with the flow diagram obtained using the Bethe-ansatz [34]. Notice that the fundamental difference from the perturbative scaling equations (21) is the Γ -function in the denominator of our flow equation for $\beta^{-2}(\ell)$. Therefore $\beta^2 = 4\pi$ is a fixed point in our approach which will be the main difference as compared to perturbative RG. This does not come as a surprise since the flow of β^2 followed from higher-order terms in the commutator $[\eta(B), H_{\text{int}}(B)]$ in Section 3.4. However, for $\beta^2 = 4\pi$ our interaction term is quadratic if considered as an interaction term for Thirring fermions (see Section 2.3), and naturally no higher-order terms can be generated in $[\eta(B), H_{\text{int}}(B)]$. Another way of saying this is that the flow in β^2 is due to approximations in the flow equation scheme when higher-order terms are generated. No flow of β^2 can occur if the flow equations close exactly.

In both phases $\tilde{u}(\ell)$ remains finite for $\ell \rightarrow \infty$. On the other hand, one easily checks that $u(\ell)$ diverges in the strong-coupling phase and vanishes asymptotically in the weak-

coupling phase. Since $u(\ell)$ has so far only been introduced for rewriting (127), its divergence in the strong-coupling phase need not worry us here. The question of the true expansion parameter of our approach will be discussed below in Section 4.4, and we will see that this expansion parameter is *not* $u(\ell)$.

In order to analyze the phase boundaries we can expand the Γ -function in (142) around $\beta^2 = 8\pi$. In leading order this reproduces the perturbative scaling equations (21)

$$\frac{d\beta^{-2}}{d\ell} = \frac{u^2}{4\pi}, \quad \frac{du}{d\ell} = \left(2 - \frac{\beta^2}{4\pi}\right)u. \tag{146}$$

This approximation eventually breaks down in the strong-coupling phase as $\beta^2(\ell)$ flows to 4π : then (146) is not a good approximation for the true flow equation (142) anymore. Notice the sign difference from (21) because ℓ from (124) corresponds to $-\ln \Lambda$, therefore ℓ is integrated from 0 to ∞ . Our flow equation approach therefore reproduces the conventional two-loop scaling equations if we expand around $\beta^2 = 8\pi$. In this way we also reproduce the hidden SU(2)-symmetry of the sine-Gordon model for $\beta_0^2 = 8\pi(1 \pm u_0)$ mentioned in Section 2.3, although our approximation scheme does not manifestly respect this symmetry. Besides showing the consistency of our new approach with the conventional perturbative RG scheme at $\beta^2 \approx 8\pi$, we also see immediately that our flow equations reproduce the Kosterlitz–Thouless phase diagram Fig. 1 of the sine-Gordon model established with RG: in the limit of small initial u_0 and $\beta_0^2 > 8\pi(1 + u_0 + O(u_0^2))$ we flow to a weak-coupling fixed point, for $\beta_0^2 < 8\pi(1 + u_0 + O(u_0^2))$ to the strong-coupling fixed point $\beta^2(\infty) = 4\pi$. These two phases are again separated by a Kosterlitz–Thouless type transition along $\beta_0^2 = 8\pi(1 + u_0 + O(u_0^2))$. For the rest of this section we will focus on the strong-coupling phase. We will return to the weak-coupling phase in Section 4.3.

4.2.2. Low-energy effective Hamiltonian

One advantage of the flow equation scheme is that we can easily analyze the behavior of our model with the final diagonal Hamiltonian $H(B = \infty)$. However, a simpler kind of analysis is possible by identifying a low-energy effective Hamiltonian and analyzing this effective Hamiltonian. This will be done in this subsection. Our results will be confirmed by the analysis of $H(B = \infty)$ in Section 4.3 later on, but the identification of a low-energy effective Hamiltonian allows us to make contact with the conventional scaling picture, which is very useful for providing a simple coherent description of the flow equation approach in the strong-coupling phase.

Let us look at $H(B)$ for large B such that $|\beta^2(B) - 4\pi| \ll 1$. Then we can approximately set $\alpha(B) = 1$ in $H_{\text{int}}(B)$ from (130) and rewrite (128)

$$H(B) = H_{\text{eff}}(B) + H_{\text{diag}}(B), \tag{147}$$

where

$$H_{\text{eff}}(B) = \int dx \left(\frac{1}{2} \Pi^2(x) + \frac{1}{2} \left(\frac{\partial \phi}{\partial x} \right)^2 \right) + \frac{\tilde{u}(B)}{a} \sum_k v(B; k) (P_1^\dagger(k) P_2(k) + P_2^\dagger(k) P_1(k)). \tag{148}$$

Now for $\alpha = 1$ the creation and annihilation operators $P_j(k)$, $P_j^\dagger(k)$ from (93) obey fermionic anticommutation relations (A20)

$$\{P_j^\dagger(k), P_j(k')\} = \delta_{kk'} \frac{L}{2\pi}, \quad \{P_j^\dagger(k), P_j^\dagger(k')\} = \{P_j(k), P_j(k')\} = 0. \quad (149)$$

One could also rewrite the kinetic term H_0 in terms of these fermions and would then arrive at a noninteracting Thirring model (26) with a nonlocal mass term as the low-energy effective Hamiltonian in the strong-coupling phase. However, we can also analyze the spectrum of our low-energy effective Hamiltonian $H_{\text{eff}}(B)$ directly by working out the following commutators

$$\begin{aligned} [H_{\text{eff}}(B), P_1^\dagger(k)] &= k P_1^\dagger(k) + \frac{\tilde{u}(B)}{a} v(B; k) P_2^\dagger(k), \\ [H_{\text{eff}}(B), P_2^\dagger(k)] &= -k P_2^\dagger(k) + \frac{\tilde{u}(B)}{a} v(B; k) P_1^\dagger(k) \end{aligned} \quad (150)$$

leading to the dispersion relation

$$E_k = \sqrt{k^2 + \left(\frac{\tilde{u}(B)}{a} v(B; k)\right)^2}. \quad (151)$$

This dispersion relation describes the single-particle/hole excitation spectrum of the full Hamiltonian $H(B)$ for momenta $|k| \ll 1/\sqrt{B}$: according to (134) the terms in $H_{\text{diag}}(B)$ corresponding to such momenta are only generated for even larger B , therefore we can neglect the effect of $H_{\text{diag}}(B)$ for excitations with $|k| \ll 1/\sqrt{B}$. In this limit we also find the initial value $v(B; k) = 1$ unchanged according to (133). Summing up, in the limit $k \rightarrow 0$ the dispersion relation for single-particle/hole excitations in the strong-coupling phase has the form $\pm E_k$ with

$$E_k = \sqrt{k^2 + M^2} \quad (152)$$

and the mass

$$M = \frac{\tilde{u}(\ell = \infty)}{a}. \quad (153)$$

Eq. (152) is also the form expected from exact methods using integrability [30]. Eq. (153) is a key result in this work since it describes the relation between the running coupling and the generated mass term in the strong-coupling regime.

We observe that the finiteness of the running coupling $\tilde{u}(\ell)$ in (148) in the limit $\ell \rightarrow \infty$ is of fundamental importance in the flow equation scheme since $\tilde{u}(\infty)$ sets the generated mass gap in the spectrum. Via (143) we can also establish the following expression for the “usual” running coupling $u(\ell)$ in the language of the scaling equations (142). In the limit of $\ell \rightarrow \infty$ one finds

$$u(\ell) = a M e^\ell. \quad (154)$$

Since $\Lambda_B \propto B^{-1/2}$ plays the role of an effective UV-cutoff generated by the flow equations, this means that the dimensionless parameter $u(\Lambda_B)$ diverges simply as the mass M divided

by the effective cutoff Λ_B

$$u(B) \propto \frac{M}{\Lambda_B}, \tag{155}$$

which allows a simple physical picture of the diverging $u(B)$ in the strong-coupling phase. Again, this does not imply the breakdown of our approach since $u(B)$ is not the expansion parameter in our approach (see Section 4.4 below).

4.2.3. *Scaling behavior of the mass gap*

We will now analyze the behavior of the single-particle/hole mass M in various regimes and compare this with results obtained with other methods. First we concentrate on the scaling behavior in the limit $u_0 \rightarrow 0$ as this can be derived analytically: according to (154) it amounts to finding the scaling invariant

$$I(\ell) = e^{-\ell} f(u(\ell), \beta^2(\ell)) \tag{156}$$

with some suitable function $f(u, \beta^2)$ such that

$$\frac{dI(\ell)}{d\ell} = 0 \tag{157}$$

along the flow generated by (142). Like in the conventional scaling analysis the mass M is then given by

$$M \propto f(u_0, \beta_0^2)/a. \tag{158}$$

One finds the same behavior as in two-loop order in Section 2.2. For example, for fixed $\beta_0^2 < 8\pi$ and $u_0 \rightarrow 0$ one can easily check that $f(u, \beta^2) = u^{1/(2-\beta^2/4\pi)}$ gives a scaling invariant up to terms in second order

$$\frac{dI(\ell)}{d\ell} = I(\ell) \times O\left(\left(\frac{u(\ell)}{2 - \beta^2(\ell)/4\pi}\right)^2\right) \tag{159}$$

and therefore

$$M \propto u_0^{1/(2-\beta_0^2/4\pi)} / a \tag{160}$$

in agreement with (22). Likewise one also finds the scaling behavior (23) and (24) since we could reproduce the perturbative RG-equations (146) in the vicinity of $\beta^2 = 8\pi$ within our flow equation approach.

Since we find agreement in two-loop order, it is of some interest to also compare with higher loop calculations [20]. For simplicity we focus on the mass gap along S_- in Fig. 1, that is for $\beta_0^2 = 8\pi(1 - u_0)$ in the limit $u_0 \rightarrow 0$. We write $\beta^2(\ell) = 8\pi(1 - v(\ell))$ and expand (138) and (139) up to third order in u and v

$$\frac{dv}{d\ell} = 2u^2 - 4(1 + \gamma)u^2v, \tag{161}$$

$$\frac{du}{d\ell} = 2uv - 4\left(\frac{\pi}{4} - \frac{\gamma}{2} - \frac{1}{2} \ln 8\right)u^3, \tag{162}$$

where $\gamma \approx 0.577$ is Euler’s constant. It is straightforward to derive the scaling invariant from these equations and one finds

$$M \propto u_0^\tau \exp\left(-\frac{1}{2u_0}\right) / a \tag{163}$$

with

$$\tau = \frac{1 - \ln 8 + \pi/2}{3} \approx 0.16. \tag{164}$$

This should be compared with the three loop result (25) [20] with the correct exponent $\tau_{\text{RG}} = 1/2$.⁵ We see that the present order of our flow equation expansion is correct up to two loop order and deviates if compared with three loop RG. This is not surprising since we have not systematically taken all the terms in order $\tilde{u}^3(\ell)$ into account in the present order of our flow equation scheme and there are contributions in order u^3 missing on the rhs of (162).

In general no closed analytical solution for the set of differential equations (142) could be found. Some numerical solutions of (142) are depicted in Fig. 4. Of course the scaling

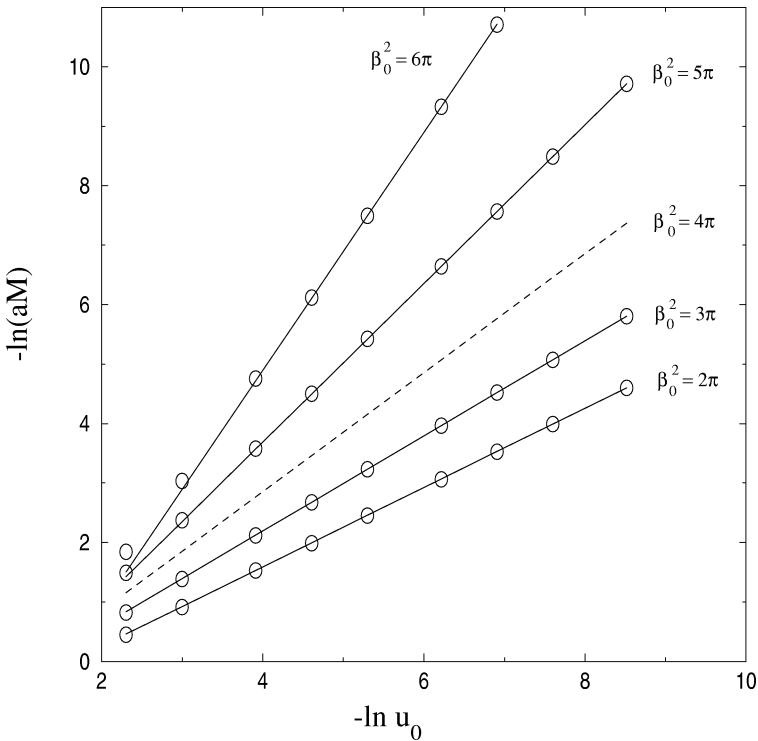


Fig. 4. Soliton mass M as a function of the coupling constant for various values of β_0^2 : the full lines are constrained fits of the power law behavior $aM \propto u_0^{1/(2-\beta_0^2/4\pi)}$ from the exact solution Refs. [17] to the flow equation results (open circles) with the proportionality constant being fitted. The dashed line is the case $\beta_0^2 = 4\pi$ where the flow equation approach agrees trivially (see text).

⁵ The deviation from the result for τ in Ref. [16] occurs because the term in order u^3 in (139) was neglected there.

behavior (160) is reproduced by these numerical solutions as can be seen in Fig. 4. Finally for $\beta_0^2 = 4\pi$ one can easily prove $M = u_0/a$ exactly using the above flow equations as should be expected since our scheme becomes exact in this case.

4.3. Properties of $H(B = \infty)$

Since the flow equation procedure diagonalizes the sine-Gordon Hamiltonian, we can not only learn something about the mass gap in the spectrum, but analyze the entire dispersion relation throughout the crossover region. The final Hamiltonian takes the structure

$$H(B = \infty) = H_0 + H_{\text{diag}}(B = \infty) \tag{165}$$

with

$$H_0 = \int dx \left(\frac{1}{2} \Pi^2(x) + \frac{1}{2} \left(\frac{\partial \phi}{\partial x} \right)^2 \right), \tag{166}$$

$$H_{\text{diag}}(B = \infty) = \sum_{k>0} \omega(B = \infty; k) (P_1(-k)P_1^\dagger(-k) + P_1^\dagger(k)P_1(k) + P_2^\dagger(-k)P_2(-k) + P_2(k)P_2^\dagger(k)) \tag{167}$$

and $P_j(k)$ defined in (93). Notice that $[H_0, H_{\text{diag}}(B = \infty)] = 0$ and $H(B = \infty)|\Omega\rangle = 0$. Using (A26) and (87) (see also the reasoning below (89)) and the normalization (88) one finds the following single-particle/hole excitation spectrum of $H(B = \infty)$:

- Soliton (particle) excitations with excitation energy E_k :

$$P_1^\dagger(k)|\Omega\rangle \quad \text{for } k > 0,$$

$$P_2^\dagger(k)|\Omega\rangle \quad \text{for } k < 0.$$

- Antisoliton (hole) excitations with excitation energy $-E_k$:

$$P_1(k)|\Omega\rangle \quad \text{for } k < 0,$$

$$P_2(k)|\Omega\rangle \quad \text{for } k > 0.$$

The dispersion relation E_k is given by

$$E_k = |k| + \omega(B = \infty; |k|). \tag{168}$$

In order to find $\omega(B = \infty; k)$ we next have to solve the system of Eqs. (133) and (134). A closed analytical solution has not been possible except for the trivial case $\beta_0^2 = 4\pi$ where one reproduces (31) exactly. However, we will see below that the flow of $\omega(B; k)$ from its initial value 0 to $\omega(B = \infty; k)$ occurs on the B -scale B_k (91) and is negligible for $B \ll B_k$ or $B \gg B_k$. We can therefore to a good approximation replace $\alpha(B)$ and $\tilde{u}(B)$ in (134) by its values for $B = B_k$ and consider them as constants. Also one can verify numerically that the term in the differential equation proportional to $\sin(\pi\alpha^2)$ changes the dispersion relation (168) only in relative order 1% for $\beta_0^2 \geq 4\pi$ (for $|k/M| < 5$ it, e.g.,

affects $\omega(B = \infty; k)$ less than 2%). In order to gain some first analytical insight we can neglect it. Notice that this approximation becomes exact in the low-energy limit in the strong-coupling phase since $\alpha^2(B) \xrightarrow{B \rightarrow \infty} 1$. We arrive at ($k > 0$)

$$\frac{\partial v(B; k)}{\partial B} = -4k^2 v(B; k) - 4k \omega(B; k) v(B; k), \tag{169}$$

$$\frac{\partial \omega(B; k)}{\partial B} = 4k v^2(B; k) c_k \tag{170}$$

with

$$c_k = -\frac{\cos(\pi \alpha^2(B_k))}{\Gamma^2(\alpha^2(B_k))} \frac{\tilde{u}^2(B_k)}{a^2} |ak|^{2\alpha^2(B_k)-2}. \tag{171}$$

Now this approximated system of flow equations can be solved easily. One finds for $0 \geq c_k > -k^2$

$$\omega(B; k) = -k + \sqrt{k^2 + c_k} \coth\left(4k\sqrt{k^2 + c_k} B + \operatorname{arccoth}\left(\frac{k}{\sqrt{k^2 + c_k}}\right)\right), \tag{172}$$

and for $c_k \geq 0$

$$\omega(B; k) = -k + \sqrt{k^2 + c_k} \tanh\left(4k\sqrt{k^2 + c_k} B + \operatorname{arctanh}\left(\frac{k}{\sqrt{k^2 + c_k}}\right)\right). \tag{173}$$

In both cases one obtains

$$\omega(B = \infty; k) = -k + \sqrt{k^2 + c_k}. \tag{174}$$

In the case $c_k \leq -k^2$ the solution for $\omega(B; k)$ diverges as $B \rightarrow \infty$. For small initial couplings u_0 this scenario can according to (171) only occur for $\alpha^2(B = 0) < 1/2$. This just defines our permissible range of parameters $\beta_0^2 \geq 2\pi$ as mentioned above. From (172) and (173) we can also read of the justification for our above approximation in the system of differential equations: nearly all the flow from $\omega(B = 0; k) = 0$ to $\omega(B = \infty; k)$ occurs on the scale $B \approx [4k\sqrt{k^2 + c_k}]^{-1} \approx B_k$ with B_k from (91). One can verify numerically that for $\beta_0^2 \geq 4\pi$ and $|k| < 3\tilde{u}(\infty)/a$ the solution (174) of the approximated flow equations agrees to within 20% with the full numerical solution of Eqs. (133) and (134) and becomes exact for $|k| \ll \tilde{u}(\infty)/a$.

Putting everything together the dispersion relation is

$$E_k = \sqrt{k^2 - \cos(\pi \alpha^2(B_k)) \left(\frac{1}{\Gamma(\alpha^2(B_k))} \frac{\tilde{u}(B_k)}{a} |ak|^{\alpha^2(B_k)-1}\right)^2}. \tag{175}$$

In the low-energy limit the dispersion relation (175) takes different forms in the weak- and strong-coupling phases:

- Weak-coupling phase: here $\alpha^2(B = \infty) \geq 2$ and we find for $|k| \ll \tilde{u}(\infty)/a$

$$E_k = |k| \sqrt{1 - \cos(\pi \alpha^2(\infty)) \left(\frac{1}{\Gamma(\alpha^2(\infty))} \tilde{u}(\infty) |ak|^{\alpha^2(\infty)-2}\right)^2}, \tag{176}$$

that is a gapless spectrum with $E_k = |k|$ for $k \rightarrow 0$.

- Strong-coupling phase: here $\alpha^2(B = \infty) = 1$ and we find for $|k| \ll \tilde{u}(\infty)/a$

$$E_k = \sqrt{k^2 + \left(\frac{\tilde{u}(\infty)}{a}\right)^2}. \tag{177}$$

This agrees with the result (152) obtained from the effective Hamiltonian analysis in Section 4.2.2, that is we find a gapped spectrum with the mass $M = \tilde{u}(\infty)/a$.

One can verify numerically that in the strong-coupling phase for $\beta_0^2 \geq 4\pi$ the full dispersion relation obtained by solving (133) and (134) is very accurately described by $\sqrt{k^2 + M^2}$ even in the crossover region: in the small coupling limit $|u_0| \ll 1$ there are β_0 -dependent universal corrections in the crossover region $k = O(M)$ that vanish for $\beta_0^2 \rightarrow 4\pi$ and reach at most 3% (for $\beta_0^2 = 8\pi$).⁶ The respective scaling forms of the dispersion relation are depicted in Fig. 5.

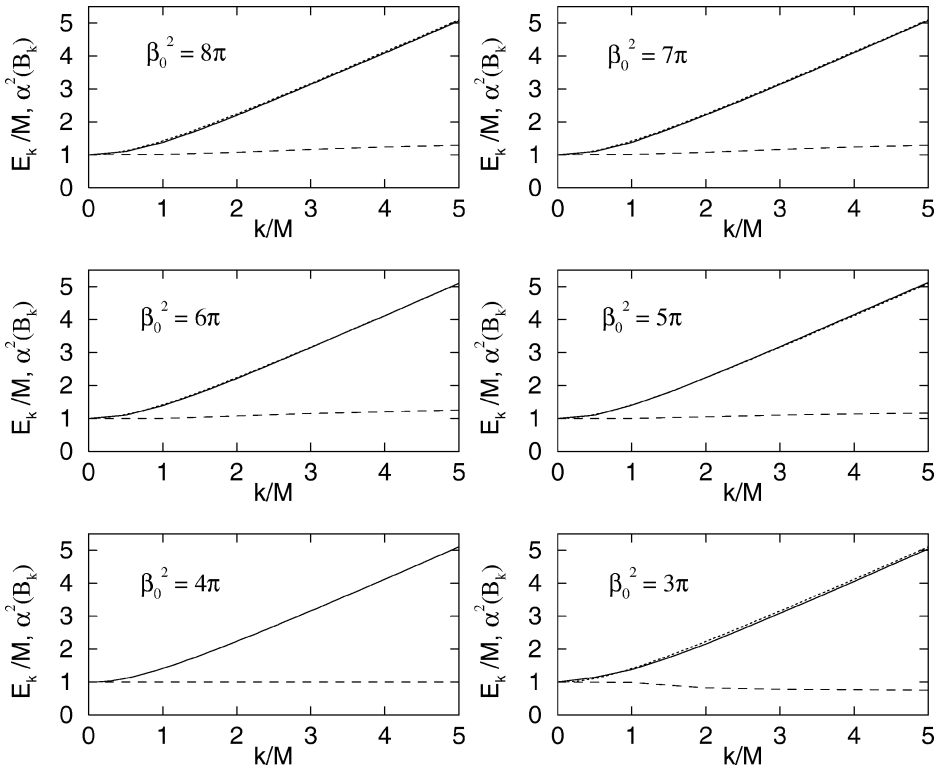


Fig. 5. Universal scaling limit for the dispersion relation E_k and the scaling dimension of the soliton excitations obtained by numerical solution of (133) and (134): the full lines depict E_k , the dotted lines $\sqrt{k^2 + M^2}$ for comparison, and the dashed lines the scaling dimension $\alpha^2(B_k)$ corresponding to the resp. wavevector.

⁶ Such small corrections might be expected from the exact results for the one-dimensional spin-1/2 XYZ-chain in Ref. [30], where the form (177) holds *exactly* also in the crossover region. However, a strict comparison with [30] is difficult since there are nontrivial renormalization subtleties in mapping the continuum sine-Gordon model to the discrete spin chain (in this context see, e.g., Ref. [31]).

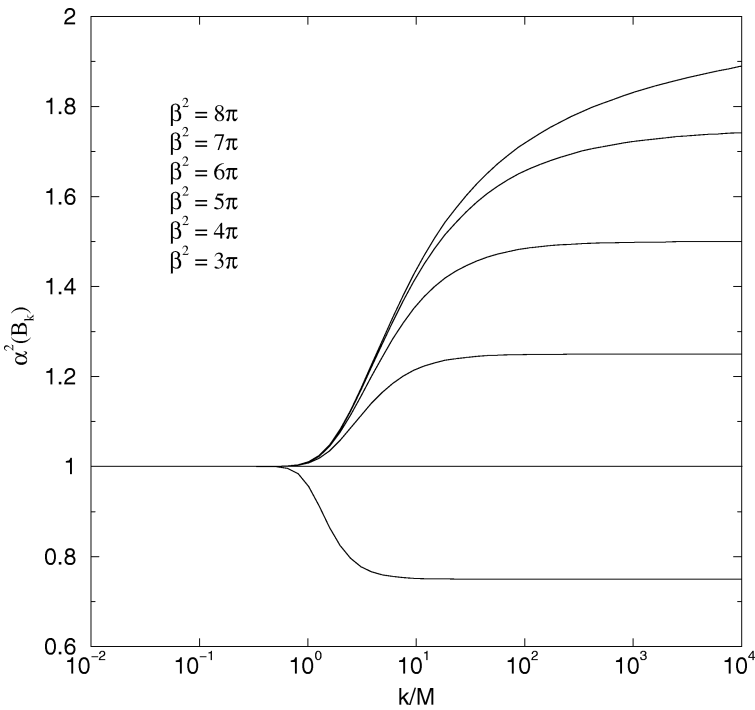


Fig. 6. Universal curves for the effective scaling dimension $\alpha^2(B_k)$ corresponding to a soliton excitation with wavevector k in the strong-coupling phase. The curves are from top to bottom for $\beta_0^2 = 8\pi, 7\pi, 6\pi, 5\pi, 4\pi, 3\pi$.

Notice that according to (93) the scaling dimension of our single-particle/hole excitations *varies* continuously along these dispersion curves, see Figs. 5 and 6. This describes the “dressing” of the single-particle/hole excitations with interactions, leading to a change in statistics. In the strong-coupling phase one finds the initial scaling dimension $\alpha(0)$ for excitations with large momenta $|k| \gg M$, and the low-energy effective Thirring fermions with $\alpha(\infty) = 1$ for small momenta $|k| \ll M$. This is consistent with the exact S -matrix results by Zamolodchikov [18] discussed in Section 2.3. Also notice that our elementary excitations in this section are described with respect to a transformed basis since $H(B = \infty)$ and $H(B = 0)$ are related by a complicated unitary transformation.

Finally let us look at the solution of Eqs. (133) and (134) for initial parameters $\beta_0^2 < 4\pi$. We have seen above that the differential equation for $\omega(B; k)$ leads to divergences for $k \rightarrow 0$ if $\alpha_0^2 < 1/2$.⁷ In other words the $\cos(\beta_0\phi(x))$ -term becomes too relevant for our flow equation approach in its present form for $\beta_0^2 < 2\pi$. This is the reason why the parameter space of the sine-Gordon model that we can deal with in this paper is *restricted*

⁷ In fact the $\sin(\pi\alpha^2)$ -term in (134) already leads to IR-problems for $\alpha_0^2 < 1$. The source of this problem is related to the breakdown at $\alpha_0^2 = 1/2$ and can be resolved in a likewise manner as will be shown in a subsequent publication: the $\sin(\pi\alpha^2)$ -terms turn out to be generally unimportant and we can safely neglect them in our present discussion also for $\alpha_0^2 < 1$.

to $\beta_0^2 \geq 2\pi$. In the interval $2\pi \leq \beta_0^2 < 4\pi$ our approximations become exact in the limit $\beta_0^2 \rightarrow 4\pi$ and, according to the observations above, eventually break down for $\beta_0^2 < 2\pi$. We will investigate the accuracy of our approximations in more detail in the following section.

4.4. Approximations and expansion parameter

Both during the flow and for the analysis of the final diagonal Hamiltonian we have neglected the terms in $H_{\text{res}}(B)$ in (128). For any given B -scale these terms are more irrelevant by at least two spatial derivatives than the interaction term $H_{\text{int}}(B)$. Our approximations are therefore similar to the expansions in renormalization approaches. To judge the accuracy of our approximations in more detail it is important to study the prefactors of these terms, that is to find the expansion parameter of our approach. Since $H_{\text{int}}(B)$ is treated as the perturbing term, we can do this easily by comparing it with H_0 , e.g., from the dispersion relation (175) one sees that on the momentum scale k the effect of $H_{\text{int}}(B)$ as compared to H_0 is

$$\frac{|ak|^{\alpha^2(B_k)} \tilde{u}(B_k)/a}{|k|} \propto \tilde{u}(B_k) \left(\frac{\sqrt{B_k}}{a}\right)^{2-\alpha^2(B_k)} = u(B_k), \tag{178}$$

where we have used (141). Not surprisingly the expansion parameter seems to be the running coupling constant $u(B)$ like in perturbative RG. According to the systems of differential equations (142) this is good news in the weak-coupling phase since $u(B)$ decays to zero on small energy scales ($B \rightarrow \infty$). However, in the strong-coupling phase $u(B)$ diverges according to (154).

Still our method is a systematic approximation even in the strong-coupling phase since our solution becomes *exact* for $\beta^2 = 4\pi$. As we have seen in Section 3, our system of flow equations closes for $\beta^2 = 4\pi$ ($\alpha^2 = 1$) and *no* higher-order interactions are generated during the flow. Therefore $H_{\text{res}}(B)$ vanishes identically on this line. This remarkable observation is our main difference from perturbative RG. It is in fact even a trivial observation since according to Section 2.3 the sine-Gordon Hamiltonian becomes equivalent to a noninteracting Thirring model for $\beta^2 = 4\pi$. And a quadratic Hamiltonian can easily be solved exactly with our scheme of unitary transformations.

Therefore the true expansion parameter of our method is *necessarily* some product of $u(B)$ and $(\alpha^2(B) - 1)$. Additionally, since the vertex operators become trivial c -number terms for $\alpha^2 = 0$, the expansion parameter also contains a term $\alpha^2(B)$: one can check explicitly that the leading terms in $H_{\text{res}}(B)$ contribute like

$$g(B) \stackrel{\text{def}}{=} u^2(B)\alpha^2(B)(\alpha^2(B) - 1). \tag{179}$$

In this context also compare our analysis in Section 3.4.3 where we have seen in (75) that the R -term (that we had to treat approximately) vanishes linearly like $\alpha^2(\alpha^2 - 1)$ as $\alpha^2 \rightarrow 1$ or $\alpha^2 \rightarrow 0$.

This dimensionless combination $g(B)$ is therefore the expansion parameter of our scheme⁸ and has to remain small throughout the entire flow in order to have a systematic and controllable approximation.

In order to verify this let us first investigate how $(\alpha^2(B) - 1)$ vanishes for $B \rightarrow \infty$ in the strong-coupling phase. We define $\epsilon(\ell) \stackrel{\text{def}}{=} \alpha^2(\ell) - 1$ and approximate (138) for large ℓ yielding

$$\frac{d\epsilon(\ell)}{d\ell} = -\epsilon(\ell) a^2 M^2 e^{2\ell}, \tag{180}$$

which can be solved easily leading to

$$\epsilon(\ell) = \epsilon(\ell_0) \exp\left[-\frac{(aM)^2}{2} (e^{2\ell} - e^{2\ell_0})\right]. \tag{181}$$

This very fast decay for $\ell \rightarrow \infty$ avoids a divergence in our expansion parameter $g(\ell)$

$$g(\ell) \propto (aM)^2 \exp\left[2\ell - \frac{(aM)^2}{2} e^{2\ell}\right] \xrightarrow{\ell \rightarrow \infty} 0. \tag{182}$$

For the full flow of $g(\ell)$ one finds universal curves in the small coupling limit $u_0 \rightarrow 0$ that depend on β_0^2 . Numerical solutions for these universal curves are shown in Fig. 7. The fact that one finds universal nonvanishing curves for $\beta_0^2 \neq 4\pi$ means that there are nonzero corrections to our present approximations even in the limit $u_0 \rightarrow 0$. This is not surprising

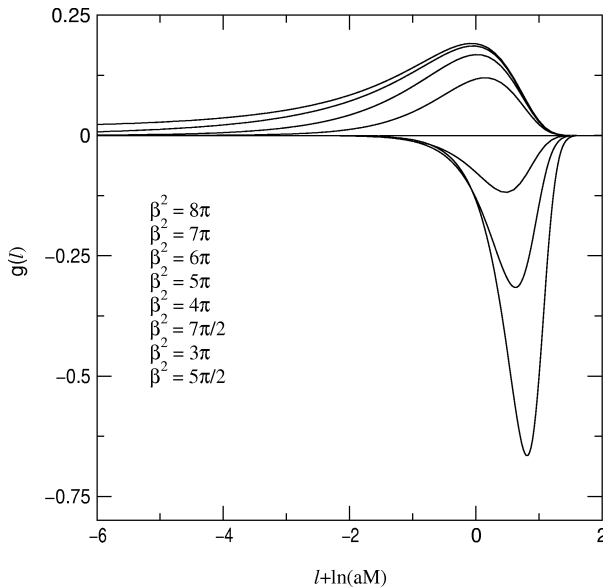


Fig. 7. Universal curves for the expansion parameter $g(\ell)$ of the flow equation approach (179). The curves are from top to bottom for $\beta_0^2 = 8\pi, 7\pi, 6\pi, 5\pi, 4\pi, 7\pi/2, 3\pi, 5\pi/2$. Notice that $g(\ell) \equiv 0$ for $\beta_0^2 = 4\pi$ since then our approach is exact.

⁸ Also the combination $g(B)u(B)$ appears, but this does not make any difference for our analysis.

due to the strong-coupling nature of our model. A precise statement about the actual size of the errors is difficult since this depends on unknown prefactors with which $g(\ell)$ enters. However, it is encouraging to observe that $|g(\ell)|$ remains relatively small throughout the entire flow for all $\beta_0^2 \geq 4\pi$. Higher-order corrections can therefore be expected to be small and are systematically obtainable in an expansion that takes more and more irrelevant terms into account in our flow equation procedure.

Finally, for $\beta_0^2 < 4\pi$ the maximum in $|g(\ell)|$ grows rapidly as β_0^2 becomes smaller as can be seen in Fig. 7. The error of our approximation therefore becomes larger as $\beta_0^2 \rightarrow 0$, which agrees with the observation in Section 4.3 that our present scheme actually breaks down for $\beta_0^2 < 2\pi$. This is not unexpected since the perturbing $\cos(\beta\phi(x))$ -term becomes more and more relevant for small β_0 .

5. Conclusions

In this paper we have developed a new approach [16] for solving the quantum sine-Gordon model (20)

$$H(B = 0) = \int dx \left(\frac{1}{2} \Pi^2(x) + \frac{1}{2} \left(\frac{\partial\phi}{\partial x} \right)^2 + \frac{u}{\pi a^2} \cos \left[\beta \int d\epsilon c(\epsilon) \phi(x + \epsilon) \right] \right) \tag{183}$$

by means of infinitesimal unitary transformations as introduced by Wegner [2] and Głazek and Wilson [3,4]. Within an approximation that neglected operators with larger scaling dimensions (more irrelevant terms) we obtained a flow that unitarily linked the initial Hamiltonian (183) to a diagonal Hamiltonian

$$H(B = \infty) = \int dx \left(\frac{1}{2} \Pi^2(x) + \frac{1}{2} \left(\frac{\partial\phi}{\partial x} \right)^2 \right) + \sum_{k>0} \omega(B = \infty; k) (P_1(-k) P_1^\dagger(-k) + P_1^\dagger(k) P_1(k) + P_2^\dagger(-k) P_2(-k) + P_2(k) P_2^\dagger(k)). \tag{184}$$

Here the $P_j(k)$ are soliton and antisoliton creation and annihilation operators as defined in (93). Their dispersion relation $\pm E_k$ was calculated in (175). In the small coupling limit $|u| \ll 1$ we found $E_k = \sqrt{k^2 + M^2}$ (with very small deviations from this form) in the strong-coupling phase, and a gapless spectrum $E_k = |k|$ in the weak-coupling phase. In the strong-coupling phase, our low-energy solitons and antisolitons are fermionic (compare Fig. 6) as known from the exact S -matrix solution [18]. Within our approach their mass M can be obtained by the solution of the flow equations (142)

$$\frac{d\beta^{-2}(\ell)}{d\ell} = \frac{1}{4\pi \Gamma(-1 + \beta^2(\ell)/4\pi)} u^2(\ell), \tag{185}$$

$$\frac{du}{d\ell} = \left(2 - \frac{\beta^2(\ell)}{4\pi} \right) u(\ell) \tag{186}$$

via the relation $M = e^{-\ell} u(\ell)/a$ in the limit $\ell \rightarrow \infty$. The above equations have to be integrated from their initial values for $\ell = 0$ to $\ell = \infty$. Our results for the scaling behavior of the mass agree with exact methods and the two-loop scaling analysis (compare Fig. 4). We also reproduce the phase diagram of the sine-Gordon model in our approach (see Figs. 1 and 3).

Our equations (185) and (186) are similar to the two-loop RG equations (21) *except* for the Γ -function in the denominator of (185) that makes $\beta^2 = 4\pi$ an *attractive strong-coupling fixed point* of the flow equation method (see Fig. 3). This is the main difference between our approach and perturbative RG. Since the sine-Gordon model for $\beta^2 = 4\pi$ can be interpreted as a noninteracting Thirring model, our flow equation procedure becomes exact at this point and diagonalizes the ensuing quadratic Hamiltonian easily. The expansion parameter of our approach is therefore *not* $u(\ell)$ (notice that $u(\ell)$ diverges in the strong-coupling phase as in perturbative scaling), but according to (179) the product $g(\ell) = u^2(\ell) (-1 + \beta^2(\ell)/4\pi)(\beta^2(\ell)/4\pi)$. $g(\ell)$ remains small throughout the entire flow for $\beta^2 \geq 4\pi$ (compare Fig. 7). This allows a *systematic* improvement of our present approximations by successively taking terms with larger scaling dimensions into account in our flow equation procedure. Furthermore, it allows us to conclude that our present approximation already provides a good description of the crossover region, which is notoriously difficult to study with other techniques. For example, we worked out the dispersion relation of the single-particle/hole excitations for all momenta in Fig. 5. Notice that higher-order terms in our expansion *cannot* endanger the stability of the strong-coupling fixed point.

As can be deduced from Fig. 7, our approximations become less accurate for $\beta^2 < 4\pi$ and eventually our present approach breaks down for $\beta^2 < 2\pi$ (Section 4.3). In addition, the bound states present in the spectrum for $\beta^2 < 4\pi$ according to the exact solution are absent in our solution. These bound states will be generated by interactions in H_{res} that are not included in our present approximation. Work on these issues for $\beta^2 < 4\pi$ is in progress.

To summarize, we have obtained an explicit approximate relation between the strong-coupling problem (183) and its diagonalized form (184) without using the integrable structure of the model. The method presented here provides a theoretical tool that is capable of achieving this in a systematic expansion throughout the crossover region. We have been able to carry out this program completely for $\beta^2 \geq 4\pi$, and obtained first results for $\beta^2 < 4\pi$ (where more work remains to be done, e.g., regarding the bound states). Our approach is conceptually simple since a small parameter is identified and used as an expansion parameter. It is therefore possible to study nonintegrable perturbations with our approach, and the calculation of correlation functions also seems feasible. Finally, there are various other one-dimensional strong-coupling problems, as for example the Kondo model, where the present approach should be useful [32].

Acknowledgements

The author acknowledges many valuable discussions with W. Hofstetter and D.S. Fisher. This work was supported by the Deutsche Forschungsgemeinschaft (DFG), by the SFB 484 of the DFG and by the National Science Foundation (NSF) under grants DMR 9630064, DMR 9976621 and DMR 9981283.

Appendix A. Properties of vertex operators

A.1. Operator product expansion

This appendix compiles some important properties of vertex operators. For a review of these properties see also Ref. [33].

We first want to establish a relation between the normal-ordered and the non-normal-ordered vertex operators. By definition

$$\begin{aligned} V_1(\alpha; x) &\stackrel{\text{def}}{=} : \exp \left(\alpha \sum_{p \neq 0} \frac{\sqrt{|p|}}{p} e^{-\frac{q}{2}|p| - ipx} \sigma_1(p) \right) : \\ &= \exp \left(\alpha \sum_{p > 0} \frac{\sqrt{|p|}}{p} e^{-\frac{q}{2}|p| - ipx} \sigma_1(p) \right) \\ &\quad \times \exp \left(\alpha \sum_{p < 0} \frac{\sqrt{|p|}}{p} e^{-\frac{q}{2}|p| - ipx} \sigma_1(p) \right) \end{aligned} \quad (\text{A1})$$

and next we can use the formula

$$e^A e^B = e^{C/2} e^{A+B} \quad (\text{A2})$$

with $C = [A, B]$ since C is a number and commutes with both A and B :

$$\begin{aligned} C &= \left[\alpha \sum_{p > 0} \frac{\sqrt{|p|}}{p} e^{-\frac{q}{2}|p| - ipx} \sigma_1(p), \alpha \sum_{q < 0} \frac{\sqrt{|q|}}{q} e^{-\frac{q}{2}|q| - iqx} \sigma_1(q) \right] \\ &= \alpha^2 \sum_{p > 0} \frac{e^{-a|p|}}{p}. \end{aligned} \quad (\text{A3})$$

The sum over q yields

$$C = -\alpha^2 \ln(1 - e^{-2\pi a/L}) \quad (\text{A4})$$

and in the thermodynamic limit $L \rightarrow \infty$

$$C = -\alpha^2 \ln \left(\frac{2\pi a}{L} \right). \quad (\text{A5})$$

Therefore

$$\begin{aligned}
 V_j(\alpha; x) &\stackrel{\text{def}}{=} : \exp\left(\pm\alpha \sum_{p \neq 0} \frac{\sqrt{|p|}}{p} e^{-\frac{a}{2}|p|-ipx} \sigma_j(p)\right) : \\
 &= \left(\frac{L}{2\pi a}\right)^{\alpha^2/2} \exp\left(\pm\alpha \sum_{p \neq 0} \frac{\sqrt{|p|}}{p} e^{-\frac{a}{2}|p|-ipx} \sigma_j(p)\right). \tag{A6}
 \end{aligned}$$

An important property of the Fourier-transformed vertex operators (78) is their action on the vacuum

$$\begin{aligned}
 V_1(\alpha; -k)|\Omega\rangle = V_1(-\alpha; k)|\Omega\rangle = V_2(\alpha; k)|\Omega\rangle = V_2(-\alpha; -k)|\Omega\rangle = 0 \\
 \forall k > 0. \tag{A7}
 \end{aligned}$$

This is shown easily, e.g.,

$$\begin{aligned}
 V_1(-\alpha; k)|\Omega\rangle &= \frac{1}{2\pi} \int dx e^{-ikx} V_1(-\alpha; x)|\Omega\rangle \\
 &= \frac{1}{2\pi} \int dx e^{-ikx} \exp\left(\alpha \sum_{p>0} \frac{\sqrt{|p|}}{p} e^{-\frac{a}{2}|p|-ipx} \sigma_1(p)\right) |\Omega\rangle. \tag{A8}
 \end{aligned}$$

One expands the second exponential and arrives at terms with the structure

$$\int dx e^{-ix(k+p_1+\dots+p_n)} = 0 \tag{A9}$$

since $k, p_1, \dots, p_n > 0$. Therefore

$$V_1(-\alpha; k)|\Omega\rangle = 0 \tag{A10}$$

for $k > 0$ and the analysis for the rest of (A7) proceeds likewise.

Next we want to evaluate expectation values for products of vertex operators. We look at the product

$$\begin{aligned}
 &V_1(\alpha; x) V_1(-\alpha; y) \\
 &= \exp\left(\alpha \sum_{p>0} \frac{\exp(-\frac{a}{2}|p|-ipx)}{\sqrt{|p|}} \sigma_1(p)\right) \exp\left(-\alpha \sum_{p<0} \frac{\exp(-\frac{a}{2}|p|-ipx)}{\sqrt{|p|}} \sigma_1(p)\right) \\
 &\quad \times \exp\left(-\alpha \sum_{q>0} \frac{\exp(-\frac{a}{2}|q|-iqy)}{\sqrt{|q|}} \sigma_1(q)\right) \exp\left(\alpha \sum_{q<0} \frac{\exp(-\frac{a}{2}|q|-iqy)}{\sqrt{|q|}} \sigma_1(q)\right) \tag{A11}
 \end{aligned}$$

and commute the second and third exponentials using the formula

$$e^A e^B = e^C e^B e^A \tag{A12}$$

with $C = [A, B]$ since again C is a number and commutes with both A and B :

$$\begin{aligned}
 C &= \left[-\alpha \sum_{p < 0} \frac{\exp(-\frac{a}{2}|p| - ipx)}{\sqrt{|p|}} \sigma_1(p), -\alpha \sum_{q > 0} \frac{\exp(-\frac{a}{2}|q| - iqy)}{\sqrt{|q|}} \sigma_1(q) \right] \\
 &= \alpha^2 \sum_{q > 0} \frac{\exp(-a|q| + iq(x - y))}{q} \\
 &= -\alpha^2 \ln(1 - e^{i\frac{2\pi}{L}(x-y+ia)}).
 \end{aligned} \tag{A13}$$

In the thermodynamic limit $L \rightarrow \infty$ this gives

$$e^C = \left(\frac{L/2\pi}{i(y-x) + a} \right)^{\alpha^2}. \tag{A14}$$

Therefore

$$\begin{aligned}
 V_1(\alpha; x) V_1(-\alpha; y) &= \left(\frac{L/2\pi}{i(y-x) + a} \right)^{\alpha^2} \exp\left(\alpha \sum_{p > 0} \frac{\exp(-\frac{a}{2}|p| - ipx)}{\sqrt{|p|}} \sigma_1(p) \right) \\
 &\quad \times \exp\left(-\alpha \sum_{q > 0} \frac{\exp(-\frac{a}{2}|q| - iqy)}{\sqrt{|q|}} \sigma_1(q) \right) \\
 &\quad \times \exp\left(-\alpha \sum_{p < 0} \frac{\exp(-\frac{a}{2}|p| - ipx)}{\sqrt{|p|}} \sigma_1(p) \right) \\
 &\quad \times \exp\left(\alpha \sum_{q < 0} \frac{\exp(-\frac{a}{2}|q| - iqy)}{\sqrt{|q|}} \sigma_1(q) \right).
 \end{aligned} \tag{A15}$$

From this we obtain the expectation value

$$\langle V_1(\alpha; x) V_1(-\alpha; y) \rangle = \left(\frac{L/2\pi}{i(y-x) + a} \right)^{\alpha^2}. \tag{A16}$$

A similar calculation can be done for $V_2(\alpha; x)$ and the only difference is the exchange of x and y in the denominator

$$\langle V_2(\alpha; x) V_2(-\alpha; y) \rangle = \left(\frac{L/2\pi}{i(x-y) + a} \right)^{\alpha^2}. \tag{A17}$$

The operator product expansion (OPE) for vertex operators can be deduced from (A15)

$$\begin{aligned}
 &V_1(\alpha; x) V_1(-\alpha; y) \\
 &= \left(\frac{L/2\pi}{i(y-x) + a} \right)^{\alpha^2} \exp\left(\alpha \sum_{p > 0} \frac{\exp(-\frac{a}{2}|p|)}{\sqrt{|p|}} (e^{-ipx} - e^{-ipy}) \sigma_1(p) \right) \\
 &\quad \times \exp\left(-\alpha \sum_{p < 0} \frac{\exp(-\frac{a}{2}|p|)}{\sqrt{|p|}} (e^{-ipx} - e^{-ipy}) \sigma_1(p) \right) \\
 &= \left(\frac{L/2\pi}{i(y-x) + a} \right)^{\alpha^2} \exp\left(-i\alpha(x-y) \sum_{p > 0} e^{-\frac{a}{2}|p| - ipx} \sqrt{|p|} \sigma_1(p) + O((x-y)^2) \right)
 \end{aligned}$$

$$\begin{aligned} & \times \exp\left(-i\alpha(x-y) \sum_{p<0} e^{-\frac{a}{2}|p|-ipx} \sqrt{|p|} \sigma_1(p) + O((x-y)^2)\right) \\ & = \left(\frac{L/2\pi}{i(y-x)+a}\right)^{\alpha^2} \left(1 + i\alpha(y-x) \sum_{p\neq 0} e^{-\frac{a}{2}|p|-ipx} \sqrt{|p|} \sigma_1(p) + O((x-y)^2)\right). \end{aligned} \tag{A18}$$

Higher order terms in the OPE can easily be deduced using the above scheme. These terms are less singular as $x \rightarrow y$, or, in the language of renormalization theory, they have a larger scaling dimension (are more irrelevant) and can be expressed as spatial derivatives of the bosonic field.

A similar calculation for $V_2(\alpha; x)$ gives

$$\begin{aligned} & V_2(\alpha; x) V_2(-\alpha; y) \\ & = \left(\frac{L/2\pi}{i(x-y)+a}\right)^{\alpha^2} \left(1 + i\alpha(x-y) \sum_{p\neq 0} e^{-\frac{a}{2}|p|-ipx} \sqrt{|p|} \sigma_2(p) + O((x-y)^2)\right), \end{aligned} \tag{A19}$$

again the only difference is the exchange of x and y .

It is well-known that for $\alpha = \pm 1$ the vertex operators describe fermion creation and annihilation operators. This can be checked easily by using the OPE (A18) in the anticommutator for the special case $\alpha = 1$

$$\begin{aligned} & \{V_1(1; x), V_1(-1; y)\} \\ & = \left(\frac{L/2\pi}{i(y-x)+a} + \frac{L/2\pi}{i(x-y)+a}\right) \\ & \quad \times \left(1 + i\alpha(y-x) \sum_{p\neq 0} e^{-\frac{a}{2}|p|-ipx} \sqrt{|p|} \sigma_1(p) + O((x-y)^2)\right) \\ & \stackrel{a \rightarrow 0}{=} L \delta(x-y) \left(1 + i\alpha(y-x) \sum_{p\neq 0} e^{-\frac{a}{2}|p|-ipx} \sqrt{|p|} \sigma_1(p) + O((x-y)^2)\right) \\ & = L \delta(x-y) \end{aligned} \tag{A20}$$

in the limit $a \rightarrow 0$. All higher-order terms in the OPE vanish in this limit. Likewise one finds

$$\{V_1(1; x), V_1(1; y)\} = \{V_1(-1; x), V_1(-1; y)\} \stackrel{a \rightarrow 0}{=} 0 \tag{A21}$$

and the same relations for $V_2(\pm 1; x)$.

A.2. Exchange relations

Let us look at the commutation relation of vertex operators in momentum space. These are worked out in the following for general α . For simplicity we only consider $V_1(\pm\alpha; x)$,

the calculation for $V_2(\pm\alpha; x)$ proceeds along similar lines. From the definition of the vertex operators one easily verifies the following relation

$$V_1(-\alpha; x)V_1(\alpha; y) = \frac{[-i(y-x) + a]^{\alpha^2}}{[i(y-x) + a]^{\alpha^2}} V_1(\alpha; y)V_1(-\alpha; x). \quad (\text{A22})$$

For large distances $|x - y| \gg a$ the coefficient can be well approximated by

$$\cos(\pi\alpha^2) + i \operatorname{sgn}(x - y) \sin(\pi\alpha^2), \quad (\text{A23})$$

whereas for small distances it becomes equal to 1. Now for small distances the operator product expansion for the two vertex operators can be used and it is then possible to write generally for all $x - y$

$$\begin{aligned} & V_1(-\alpha; x)V_1(\alpha; y) - \text{OPE}(x \rightarrow y) \\ &= (\cos(\pi\alpha^2) + i \operatorname{sgn}(x - y) \sin(\pi\alpha^2))(V_1(\alpha; y)V_1(-\alpha; x) - \text{OPE}(x \rightarrow y)). \end{aligned} \quad (\text{A24})$$

For our purposes here it will be sufficient to look only at the leading c -number term in the OPE (higher-orders can easily be taken into account if necessary). This is equivalent to subtracting the ground state expectation value on both sides (50). Notice that our relation “closes”

$$\begin{aligned} & *V_1(-\alpha; x)V_1(\alpha; y)* \\ &= (\cos(\pi\alpha^2) + i \operatorname{sgn}(x - y) \sin(\pi\alpha^2)) *V_1(\alpha; y)V_1(-\alpha; x)* \\ &= (\cos(\pi\alpha^2) + i \operatorname{sgn}(x - y) \sin(\pi\alpha^2)) \\ &\quad \times (\cos(\pi\alpha^2) + i \operatorname{sgn}(y - x) \sin(\pi\alpha^2)) *V_1(-\alpha; x)V_1(\alpha; y)* \\ &= *V_1(-\alpha; x)V_1(\alpha; y)*. \end{aligned} \quad (\text{A25})$$

In terms of Fourier components (78) this reads ($\alpha > 0$)

$$\begin{aligned} & *V_1(-\alpha; k_1)V_1(\alpha; k_2)* \\ &= \frac{1}{2\pi} \sum_p *V_1(\alpha; k_2 + p)V_1(-\alpha; k_1 + p)* \\ &\quad \times \int dx e^{ipx} (\cos(\pi\alpha^2) + i \operatorname{sgn}(x) \sin(\pi\alpha^2)) \\ &= \cos(\pi\alpha^2) *V_1(\alpha; k_2)V_1(-\alpha; k_1)* \\ &\quad + \sin(\pi\alpha^2) \frac{2}{\pi} \sum_{n=0}^{\infty} \frac{1}{2n+1} \\ &\quad \times \left[*V_1\left(\alpha; k_2 - \frac{2\pi}{L}(2n+1)\right)V_1\left(-\alpha; k_1 - \frac{2\pi}{L}(2n+1)\right)* \right. \\ &\quad \left. - *V_1\left(\alpha; k_2 + \frac{2\pi}{L}(2n+1)\right)V_1\left(-\alpha; k_1 + \frac{2\pi}{L}(2n+1)\right)* \right] \end{aligned}$$

$$\begin{aligned}
&= \cos(\pi\alpha^2) * V_1(\alpha; k_2)V_1(-\alpha; k_1)* \\
&\quad - \frac{1}{\pi} \sin(\pi\alpha^2) \operatorname{Re} \int dq \frac{1}{q+i\epsilon} * V_1(\alpha; k_2+q)V_1(-\alpha; k_1+q)* \\
&= -\frac{1}{\pi} \operatorname{Im} \left[e^{i\pi\alpha^2} \int dq \frac{1}{q+i\epsilon} * V_1(\alpha; k_2+q)V_1(-\alpha; k_1+q)* \right] \quad (\text{A26})
\end{aligned}$$

in the thermodynamic limit with $\lim_{\epsilon \downarrow 0}$ being understood. Likewise

$$\begin{aligned}
&*V_1(\alpha; k_1)V_1(-\alpha; k_2)* \\
&= -\frac{1}{\pi} \operatorname{Im} \left[e^{-i\pi\alpha^2} \int dq \frac{1}{q+i\epsilon} * V_1(-\alpha; k_2+q)V_1(\alpha; k_1+q)* \right]. \quad (\text{A27})
\end{aligned}$$

Notice that these relations close in k -space in the same sense as (A25). They are only “simple” for integer α^2 when the vertex operators behave as bosons or fermions: then the term proportional to $\sin(\pi\alpha^2)$ with its summation over wavevectors vanishes.

References

- [1] K.G. Wilson, *Rev. Mod. Phys.* 47 (1975) 773.
- [2] F. Wegner, *Ann. Phys. (Leipzig)* 3 (1994) 77.
- [3] S.D. Głazek, K.G. Wilson, *Phys. Rev. D* 48 (1993) 5863.
- [4] S.D. Głazek, K.G. Wilson, *Phys. Rev. D* 49 (1994) 4214.
- [5] A. Kabel, F. Wegner, *Z. Phys. B* 103 (1997) 555.
- [6] S. Kehrein, A. Mielke, *Ann. Phys. (Leipzig)* 6 (1997) 90.
- [7] S. Kehrein, A. Mielke, *J. Stat. Phys.* 90 (1998) 889.
- [8] S. Kehrein, A. Mielke, *Ann. Phys. (NY)* 252 (1996) 1.
- [9] A. Mielke, *Ann. Phys. (Leipzig)* 6 (1997) 215.
- [10] A. Mielke, *Europhys. Lett.* 40 (1997) 195.
- [11] M. Ragwitz, F. Wegner, *Eur. Phys. J. B* 8 (1999) 9.
- [12] J. Stein, *Europhys. Lett.* 50 (2000) 68.
- [13] C. Knetter, G. Uhrig, *Eur. Phys. J. B* 13 (2000) 209.
- [14] F. Wegner, in: *Les Houches, France, 1997, New Non-Perturbative Methods and Quantization on the Light Cone*, Vol. 8, Editions de Physique/Springer, 1998, p. 33.
- [15] S. Głazek, K.G. Wilson, *Phys. Rev. D* 57 (1998) 3558.
- [16] S. Kehrein, *Phys. Rev. Lett.* 83 (1999) 4914.
- [17] E.K. Sklyanin, L.A. Takhtadzhyan, L.D. Faddeev, *Teor. Mat. Fiz.* 40 (1979) 194; *Theor. Math. Phys.* 40 (1979) 688.
- [18] A.B. Zamolodchikov, *Pisma Zh. Eksp. Teor. Fiz.* 25 (1977) 499; *JETP Letters* 25 (1977) 468.
- [19] J. Sólyom, *Adv. Phys.* 28 (1979) 201.
- [20] D.J. Amit, Y.Y. Goldschmidt, G. Grinstein, *J. Phys. A* 13 (1980) 585.
- [21] P.B. Wiegmann, *J. Phys. C* 11 (1978) 1583.
- [22] A.O. Gogolin, A.A. Nersesyan, A.M. Tsvelik, *Bosonization and Strongly Correlated Systems*, Cambridge University Press, Cambridge, 1998.
- [23] H. Bergknoff, H.B. Thacker, *Phys. Rev. D* 19 (1979) 3666.
- [24] S. Coleman, *Phys. Rev. Lett. D* 11 (1975) 2088.
- [25] S. Mandelstam, *Phys. Rev. D* 11 (1975) 3026.
- [26] G. Toulouse, *C. R. Acad. Sci. Paris* 268 (1969) 1200.
- [27] J. Stein, *Eur. Phys. J. B* 12 (1999) 5.
- [28] D. Cremers, A. Mielke, *Physica D* 126 (1999) 123.

- [29] A. Luther, V.J. Emery, Phys. Rev. Lett. 33 (1974) 589.
- [30] J.D. Johnson, S. Krinsky, B. McCoy, Phys. Rev. A 8 (1973) 2526.
- [31] A. Luther, I. Peschel, Phys. Rev. B 12 (1975) 3908.
- [32] W. Hofstetter, S. Kehrein, cond-mat/0008242.
- [33] J. von Delft, H. Schoeller, Ann. Phys. (Leipzig) 4 (1998) 225.
- [34] G.I. Japaridze, A.A. Nersesyan, P.B. Wiegmann, Nucl. Phys. B 230 [FS10] (1984) 511.